Journal of Gastroenterology and Hepatology

JGHF

doi:10.1111/j.1440-1746.2010.06248.x

HEPATOLOGY

Carbon dioxide-based portography: An alternative to conventional imaging with the use of iodinated contrast medium

Hitoshi Maruyama, Hidehiro Okugawa, Hiroyuki Ishibashi, Masanori Takahashi, Satoshi Kobayashi, Hiroaki Yoshizumi and Osamu Yokosuka

Department of Medicine and Clinical Oncology, Chiba University Graduate School of Medicine, Chiba, Japan

Key words
carbon dioxide, contrast medium, portography, portal hypertension.

Accepted for publication 20 December 2009.

Correspondence
Hitoshi Maruyama, Department of Medicine and Clinical Oncology, Chiba University Graduate School of Medicine, 1-8-1, Inohana, Chuou-ku, Chiba, 260-8670, Japan. Email: maru-cib@umin.ac.jp

Abstract

Background and Aim: To clarify the efficacy of carbon dioxide (CO_2) as a contrast material to evaluate portal vein images by percutaneous transhepatic portography (PTP).

Methods: Twenty patients (38–76 years; male 13, female 7) with chronic liver diseases were the subjects of this prospective study. Portal venous opacification by PTP was compared between CO_2-based images and iodinated contrast medium (ICM)-based images by two independent reviewers, according to the three-grade scoring; 0 for none, 1 for weak and 2 for sufficient.

Results: Total scores of extrahepatic portal veins (137 for CO_2, 93 for ICM), collateral vessels (64 for CO_2, 60 for ICM) and intrahepatic portal veins (69 for CO_2, 76 for ICM) were not statistically significant between CO_2-based and ICM-based images ($P = 0.0623$). Sufficient opacification of superior mesenteric vein was more frequent on CO_2-based images (none 0, weak 4, sufficient 16) than ICM-based images (none 19, weak 0, sufficient 1; $P < 0.0001$). The score was not statistically significant between CO_2-based and ICM-based images in portal trunk, splenic vein, inferior mesenteric vein and other collateral vessels. Although opacification grade in the intrahepatic left portal vein was not statistically significant between CO_2-based and ICM-based images ($P = 0.1515$), weak opacification was significantly frequent on CO_2-based images (weak 10, sufficient 10) compared to ICM-based images (weak 0, sufficient 20; $P = 0.0003$) in the intrahepatic right portal vein. Inter-reviewer agreement was excellent between the two reviewers for CO_2-based images (kappa = 0.913) and ICM-based images (kappa = 0.924).

Conclusions: Carbon dioxide may be a first-line contrast material for evaluating portal vein images by PTP.

Introduction

Because of the development of high-performance medical accessories, interventional radiology has gained wide popularity and extended application. As a consequence, iodinated contrast medium (ICM) has been frequently used via intravascular injection for diagnosis and treatment procedures in clinical practice. However, as ICM sometimes causes severe adverse events such as renal toxicity and/or allergy, reduction in the frequency of ICM use is now occurring worldwide.[1,2]

Carbon dioxide (CO_2) is recognized as an effective contrast material for vascular enhancement during angiography, because of its safety, low viscosity, stable effect and low cost, based on a prevalence of the digital subtraction angiography (DSA) system.[3,4] Previous studies have shown the clinical utility of splenoportography and wedge hepatic venography with the use of CO_2 to present portal vein images.[5–8] However, these methods have some limitations, as they do not allow the treatment of embolization for collateral vessels or dilation for stenotic vessels. Furthermore, they have the disadvantage of being unable to measure portal pressure, as it is not provided by splenoportography and nor, in the case of pre-sinusoidal obstruction, by wedge hepatic venography.[9]

Percutaneous transhepatic portography (PTP) is a well-established angiographic technique that provides a detailed portal venous appearance and measurement of portal venous pressure.[10–12] Although its invasive aspect may be a shortcoming, PTP still remains an essential procedure especially in treatment-required cases.[5,13,14] However, the efficacy of the use of CO_2 to evaluate the portal venous appearance during the PTP process has not been fully discussed.

Based on these backgrounds, we have designed this prospective study to compare the grade of opacification of each of the portal veins and collateral vessels between CO_2-based and ICM-based portograms. The aim of this study was to clarify the efficacy of

CO_2 as a contrast material to evaluate portal vein images as an alternative to ICM during the PTP procedure.

Methods

Patients

Between February 2007 and August 2009, a prospective study was performed at the Chiba University Hospital, Chiba, Japan, after the approval of the ethics committee, with informed written consent from all patients. Inclusion criteria were: (i) cirrhosis or idiopathic portal hypertension (IPH) patients just after effective treatment of esophageal varices by endoscopic sclerotherapy; (ii) cirrhosis or IPH patients scheduled to undergo radiological treatment of gastric fundal varices diagnosed by endoscopy; and (iii) patients with scheduled PTP to examine portal hemodynamics informative for subsequent clinical management. Exclusion criteria were: (i) patients with liver dysfunction of Child–Pugh C grade not being candidates for variceal treatment; (ii) patients with ascites, portal vein thrombosis or focal hepatic lesion on sonogram; (iii) patients with severe impaired coagulation, platelet count less than 50 000/μL or prothrombin time less than 40%.

The subjects were 20 consecutive patients (age: 38–76 years, 59 ± 11; male 13, female 7), 16 with cirrhosis (age: 38–76 years, 59 ± 11; male 10, female 6) and 4 with IPH (age: 49–69, 59 ± 10; male 3, female 1). Thirteen patients had esophageal varices that were effectively treated and seven patients had gastric fundal varices deserving to be treated (elective treatment in 5, prophylactic treatment in 2). At the time of PTP, patients with suspected IPH or with negative findings of hepatitis B or C virus infection received concomitant hepatic venography. Free and wedged hepatic venous pressures were measured to examine for the presence of the pathophysiology of pre-sinusoidal block, which is a characteristic finding in IPH. Histological diagnosis of the liver was made in all 20 patients by liver biopsy after PTP: non-cirrhotic specimens in 4, cirrhosis in 16 with etiology of hepatitis C virus in 6, alcohol abuse in 4, autoimmune in 3, hepatitis B virus in 1, non-alcoholic steatohepatitis in 2. In the cirrhosis patients, the degree of liver function reserve as classified by Child-Pugh scoring system was A in 10 and B in 6. Diagnosis of IPH for the remaining 4 patients was based on blood tests, hepatic venography and histology from biopsy specimens in all patients according to the general rules for the study of portal hypertension.[15]

Percutaneous transhepatic portography

The angio machine used in this study was Infinix Celeve-VB110A/J1 (Toshiba, Tokyo, Japan) with the standard DSA system. Portal vein catheterization was performed by means of an ultrasound-guided procedure with regional anesthesia and intravenous sedation in the supine position. Then, a 4-Fr catheter (SV-2, Hanako Medical, Saitama, Japan) was advanced to the splenic hilum by plastic-coated guidewire (Radifocus guidewire M, 0.035; Terumo, Tokyo, Japan). The settings of the angio machine were 82 kV, 630 mA, 38.00 ms and 5.0 f/s for CO_2 injection, and 82 kV, 400 mA, 55.00 ms and 3.0 f/s for ICM injection. As for the CO_2 injection, a 50-cc syringe was connected to the tank via three-way stopcock, and 40 cc of CO_2 was prepared in the syringe. Care was taken to close the tip of the syringe with the stopcock after filling of CO_2 to avoid air contamination.[16] Portograms were taken twice, firstly by CO_2 injection manually and rapidly, and secondly by ICM injection (30 mL, 5 mL/s, Omnipaque300, Daiichi-Sankyo, Tokyo, Japan) by means of a mechanical injection system (Mark V ProVis, MEDRAD, Warrendale, PA, USA). The approximate time of fluoroscopy was 5 s for CO_2 based-images and 10 s for ICM-based images from the beginning of the contrast material injection. All PTP procedures were performed by HO, HI and MT, hepatologists and radiologists with more than 7 years of experience at the time of the initial case. Complications were assessed by clinical symptoms and monitoring of vital signs including blood pressure, pulse rate, oxygen saturation, electrocardiogram and urine volume during and after the examinations. Furthermore, ultrasound observations and blood tests were added on the following day to check for adverse events; the former for ascites due to intraperitoneal bleeding from the liver surface, intrahepatic arterioportal communication resulting from the puncture, and portal vein thrombosis due to the catheterization, and the latter for liver and renal dysfunction, and anemia.

Review process of portograms

Four representative photograms of approximately maximum opacification in the intra-, and extrahepatic portal veins and collateral vessels were selected from each cine image of CO_2-based and ICM-based portograms by HM, a hepatologist and radiologist with more than 17 years of experience at the time of the initial case. These eight photograms, four CO_2-based images and four ICM-based images, were printed out and forwarded to the review process. The review was conducted for the following vessels: intrahepatic right and left portal veins, extrahepatic portal veins including portal trunk, splenic vein, superior mesenteric vein and inferior mesenteric vein, and collateral vessels including left gastric vein, posterior gastric vein, short gastric vein, and paraumbilical vein. The review criteria for portal vein findings were based on the scoring of three grades of opacification: 0 for none, 1 for weak, and 2 for sufficient.

There were two independent reviewers in our study, A (SK) and B (HY), hepatologists and radiologists with more than 9 years of experience at the time of the initial case. The review results for the opacification grade in the vessels were compared between CO_2-based images and ICM-based images. Consensual decision-making by the two reviewers was applied to lack-of-consensus review results to obtain the final score.

Statistical analysis

The Chi-square test was used for comparison of the total scores reviewed for intrahepatic portal veins, extrahepatic portal veins and collateral vessels between CO_2-based and ICM-based images, and for comparison of the differences in the grade of opacification in each vessel between ICM-based and CO_2-based images. Inter-reviewer (reviewer A *vs* B) agreement was assessed by Kappa value calculation. Agreement grade was defined as < 0.2 for poor, 0.2–0.4 for moderate, 0.4–0.6 for fair, 0.6–0.8 for good, and 0.8–1.0 for excellent. Statistical significance was taken

Journal of Gastroenterology and Hepatology **25** (2010) 1111–1116

at $P < 0.05$. Statistical analysis was performed using the Dr SPSS package (version 11.0J for Windows; SPSS Inc., Chicago, IL, USA).

Results

Comparison of portograms between CO_2-based images and ICM-based images

CO_2- and ICM-based portograms were successfully obtained in all subjects without any adverse events during and after PTP examinations (Figs. 1,2). Total scores reviewed in the extrahepatic portal veins (137 for CO_2, 93 for ICM), collateral vessels (64 for CO_2, 60 for ICM) and intrahepatic portal veins (69 for CO_2, 76 for ICM) were not statistically significant between CO_2-based and ICM-based images ($P = 0.0623$, Table 1). Inter-reviewer agreement was excellent between reviewers A and B for CO_2-based images (kappa = 0.913) and ICM-based images (kappa = 0.924).

Difference in opacification grade in each of the portal veins between CO_2-based images and ICM-based images

In the extrahepatic portal veins, the scores in the portal trunk and splenic vein were identical between CO_2-based and ICM-based images, and the scores in the inferior mesenteric vein were not statistically significant between them ($P = 0.1626$, Table 1). However, sufficient opacification of the superior mesenteric vein was more frequent on CO_2-based images (none 0, weak 4, sufficient 16) than ICM-based images (none 19, weak 0, sufficient 1; $P < 0.0001$). As for the collateral vessels, the scores in the paraumbilical vein were identical between CO_2-based and ICM-based images. In addition, the scores were not statistically significant between CO_2-based and ICM-based images in the left gastric vein ($P = 0.1889$), posterior gastric vein ($P = 0.5244$), and short gastric vein ($P = 0.6298$).

Although the opacification grade in the intrahepatic left portal vein was not statistically significant between CO_2-based images (weak 1, sufficient 19) and ICM-based images (weak 4, sufficient 16; $P = 0.1515$), weak opacification was significantly frequent on CO_2-based images (weak 10, sufficient 10) compared to ICM-based images (weak 0, sufficient 20, $P = 0.0003$) in the intrahepatic right portal vein.

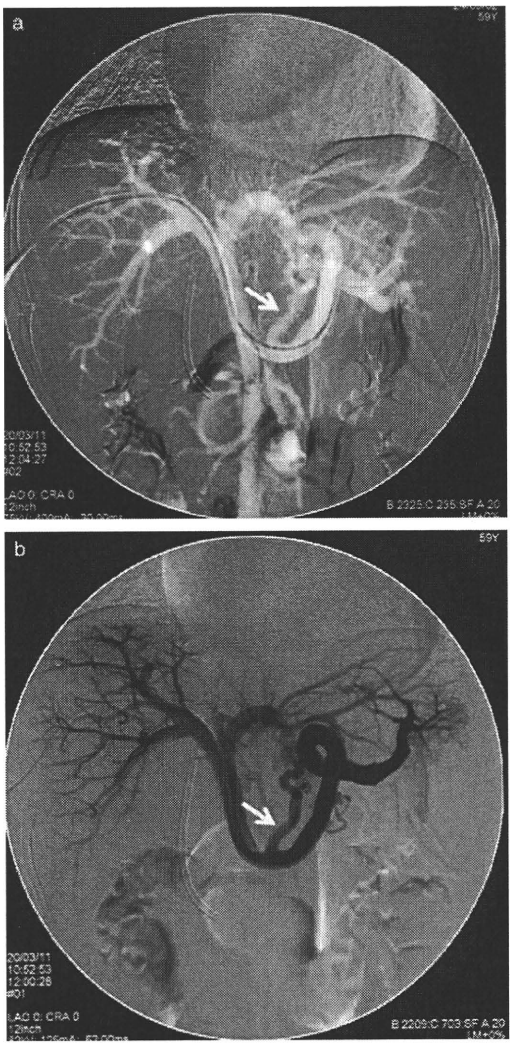

Figure 1 59-year old female, cirrhosis caused by autoimmune hepatitis, after treatment of esophageal varices. (a) CO_2-based portogram. Portal trunk, splenic vein, superior mesenteric vein, left gastric vein (arrow), and intrahepatic portal veins were sufficiently opacified. (b) ICM-based portogram. Portal trunk, splenic vein, left gastric vein (arrow), and intrahepatic portal veins were sufficiently opacified. However, superior mesenteric vein was not demonstrated on this image. CO_2, carbon dioxide; ICM, iodinated contrast medium.

Discussion

Offering technical improvement with a reduction in the incidence of adverse events is an obvious benefit for patients. Our study proved the efficacy of CO_2 as a contrast material for the evaluation of portal venous appearance during PTP examination, with the non-requirement of a mechanical power injector. CO_2-based PTP may become a standard and reliable procedure for the detailed examination of portal hemodynamics in patients with portal hypertension.

Carbon dioxide has the beneficial aspects of an intravascular rapid diffusion property as well as non-toxicity.[3,4] This diffusion factor may be the reason for the better demonstration of the superior mesenteric vein on CO_2-based images than ICM-based images, although this vessel has hepatopetal flow direction against the spreading of contrast material discharged from the splenic hilum to opacify the vessel. It should be emphasized that CO_2 allows wider visualization of the extrahepatic portal venous system under shorter fluoroscopy time than ICM, and this advantage may substantially reduce radiation exposure. However, it remains to be elucidated if CO_2 discharged from the superior mesenteric vein may provide sufficient demonstration of the splenic vein and the other collateral vessels derived from the splenic vein.

Contrast material was injected in a single uniform way in our study—30 mL of ICM and 40 cc of CO_2. The former is a standard

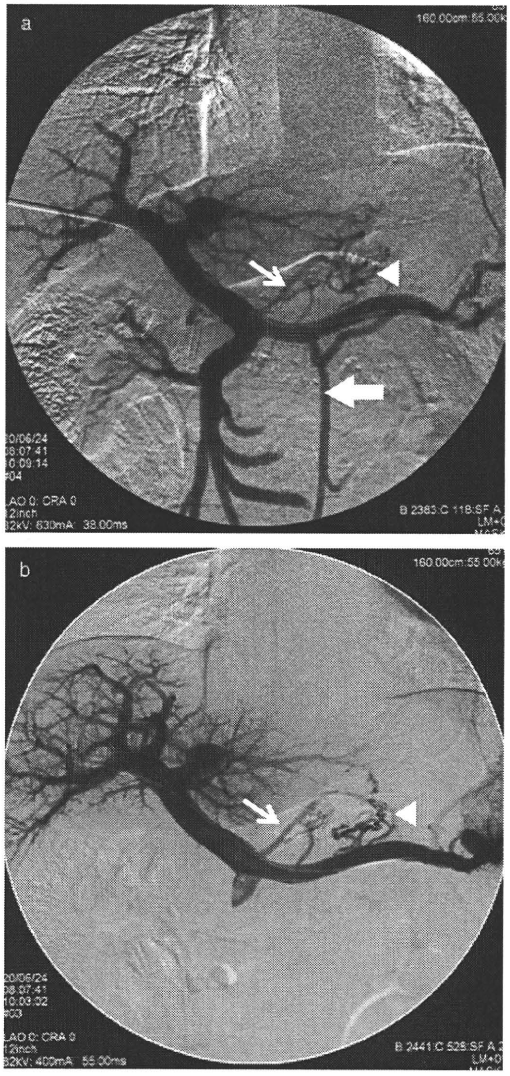

Figure 2 65-year old male, cirrhosis caused by non-alcoholic steatohepatitis, after treatment of esophageal varices. (a) CO_2-based portogram. Portal trunk, splenic vein, superior mesenteric vein, left gastric vein (arrow), posterior gastric vein (arrow head), inferior mesenteric vein (thick arrow), and intrahepatic left portal vein were sufficiently opacified. However, intrahepatic right portal vein had weak opacification on this image. (b) ICM-based portogram. Portal trunk, splenic vein, left gastric vein (arrow), posterior gastric vein (arrow head), and intrahepatic portal veins were sufficiently opacified. However, neither superior mesenteric vein nor inferior mesenteric vein was demonstrated on this image. CO_2, carbon dioxide; ICM, iodinated contrast medium.

dose in our department and in the literature,[17] and the latter was defined based on previous reports: 30–40 cc of CO_2 was given to adults in the study by Caridi *et al.*[6] and the safety of 80 cc of CO_2 for average-size patients was reported by Hawkins *et al.*[4] In addition, an actual, reasonable aspect was that the commonly available largest syringe was 50 cc in size, and the approximately 80%-filled 50-cc syringe presented an easy-handling manner for manual injection. In fact, as there were no adverse events from CO_2 injection in our study, the safety of 40 cc of CO_2 for adults was also proven. However, as the injection of a large volume of CO_2 causes displacement of blood from the right side of the heart, a serious complication called 'vapor lock', operators should be careful about the excessive use of CO_2.[4] As for the injection of CO_2, additionally, contamination with air should also be strictly avoided, especially in patients with portal hypertension, as they have portosystemic collateral vessels on one level or another. It is reported that most of the patients with gastric fundal varices had a large gastrorenal shunt, a major outflow route of varices into the inferior vena cava via the left renal vein.[18] Obviously, unnecessary injection of CO_2 should be avoided, and the volume of CO_2 might preferably be prepared based on conditions such as body mass index (BMI) of the subject and/or the vessels to be opacified.

Thanks to the development of digital technologies, non-invasive assessment with the use of ultrasound or magnetic resonance imaging (MRI) has been available for portal hemodynamics, while clinical interests of direct catheterization into the portal vein might have dropped off.[19,20] However, in spite of their benefits, these apparently convenient modalities also seem to have some disadvantages. Taourel *et al.* reported that portal velocity or flow on Doppler measurement had limited utility in predicting either hepatic venous pressure gradients or severity of liver failure in an individual patient because of the scattering of the data.[21] According to the study by Lin *et al.* three-dimensional contrast-enhanced MR portography had a limitation in the differential diagnosis of portal vein between narrowing and obstruction, although it had the advantage of detecting a small thrombus in the portal vein.[22] In addition, results obtained by ultrasound observation depend on the patient's body habitus and the operator's skill, and the generally insufficient prevalence of MRI equipment is still a problem for its widespread application. The PTP technique is directly effective for the treatment of dilatation or obstruction of impaired portal vein.[13,23–26] The use of PTP with CO_2 may continue to play an important role in the clinical management of patients with portal hypertension in spite of the invasiveness.

There were some limitations to our study. First, weak opacification in the intrahepatic right portal vein was more frequent on CO_2-based images than ICM-based images, a propensity not found in the intrahepatic left portal vein. The authors speculated that gravity might have forced CO_2 to the left portal vein branch in the supine-positioned patient because of its high buoyancy.[4] In addition, as the intrahepatic right portal vein is the farthest vessel from the catheter tip at the splenic hilum, it is open to a variety of influences of CO_2 distribution after the discharge. In any event, the CO_2-based portogram may underestimate the findings of intrahepatic right portal vein branches, though this might be resolved by changing the position of the body, placement of the catheter tip, or CO_2 volume. However, as the effects of these additional techniques have not been investigated, underestimation of intrahepatic right portal vein should be realized as a disadvantage of CO_2-based portography. Second, opacification of collateral vessels was assessed after the completion of variceal treatment in patients with esophageal varices, because evaluation of portal hemodynamics by PTP after the treatment was considered beneficial for the subsequent management of the patients.[27]

Table 1 Comparison of the grade of opacification in the portal vein between CO_2-based images and ICM-based images

	PT	SV	SMV	IMV	LGV	PGV	SGV	PUV	RPV	LPV
CO_2, A	0/0/20	0/0/20	0/4/16	7/5/8	5/7/8	9/6/5	7/10/3	17/0/3	0/10/10	0/1/19
CO_2, B	0/0/20	0/0/20	0/5/15	7/5/8	4/6/10	9/6/5	7/8/5	17/0/3	0/9/11	0/1/19
CO_2, F	0/0/20	0/0/20	0/4/16	7/5/8	4/6/10	9/6/5	7/10/3	17/0/3	0/10/10	0/1/19
	(40)	(40)	(36)	(21)	(26)	(16)	(16)	(6)	(30)	(39)
ICM, A	0/0/20	0/0/20	19/1/0	13/3/4	8/2/10	11/3/6	5/11/4	17/0/3	0/0/20	0/4/16
ICM, B	0/0/20	0/0/20	19/0/1	13/4/3	9/1/10	11/3/6	5/13/2	17/0/3	0/0/20	0/7/13
ICM, F	0/0/20	0/0/20	19/0/1	13/3/4	8/2/10	11/3/6	5/13/2	17/0/3	0/0/20	0/4/16
	(40)	(40)	(2)	(11)	(22)	(15)	(17)	(6)	(40)	(36)

Extrahepatic portal veins:
IMV, inferior mesenteric vein; PT, portal trunk; SMV, superior mesenteric vein; SV, splenic vein.
Collateral vessels:
LGV, left gastric vein; PGV, posterior gastric vein; PUV, paraumbilical vein; SGV, short gastric vein.
Intrahepatic portal veins:
LPV, intrahepatic left portal vein; RPV, intrahepatic right portal vein.
CO_2, carbon dioxide; ICM, iodinated contrast medium.
Number, none/weak/sufficient, grade of opacification reviewed by the reviewer.
Number shown in parentheses, scoring by 0 for none, 1 for weak and 2 for sufficient.
A, reviewer A; B, reviewer B; F, final review result.

Therefore, the left gastric vein, a major inflow route for esophageal varices, was in a treatment-modified status in the present study, and the effectiveness of CO_2 in demonstrating the treatment-unmodified left gastric vein, in a narrow sense, has still to be elucidated.

In conclusion, although additional study with large numbers of patients would be required to confirm our results, CO_2 may be a first-line contrast material for evaluating portal vein images by PTP, except for the visualization of intrahepatic right portal vein. The specific utility of CO_2-based portography in clinical practice still needs to be thoroughly investigated.

References

1 Waybill MM, Waybill PN. Contrast media-induced nephrotoxicity: identification of patients at risk and algorithms for prevention. *J. Vasc. Interv. Radiol.* 2001; **12**: 3–9.
2 Mehran R, Nikolsky E. Contrast-induced nephropathy: definition, epidemiology and patients at risk. *Kidney Int.* 2006; **Apr** (Suppl 100): S11–15.
3 Kerns SR, Hawkins IF. Carbon dioxide digital subtraction angiography: expanding applications and technical evolution. *AJR Am. J. Roentgenol.* 1995; **164**: 735–41.
4 Hawkins IF, Caridi JG. Carbon dioxide (CO_2) digital subtraction angiography: 26-year experience at the University of Florida. *Eur. Radiol.* 1998; **8**: 391–402.
5 Burke CT, Weeks SM, Mauro MA, Jaques PF. CO_2 Splenoportography for evaluating the splenic and portal veins before and after liver transplantation. *J. Vasc. Interv. Radiol.* 2004; **15**: 1161–5.
6 Caridi JG, Hawkins Jr. IF, Cho K *et al.* CO_2 Splenoportography: preliminary results. *AJR Am. J. Roentgenol.* 2003; **180**: 1375–8.
7 Maleux G, Nevens F, Heye S, Verslype C, Marchal G. The use of carbon dioxide wedged hepatic venography to identify the portal vein: comparison with direct catheter portography with iodinated contrast medium and analysis of predictive factors influencing level of opacification. *J. Vasc. Interv. Radiol.* 2006; **17**: 1771–9.
8 Debernardi-Venon W, Bandi J-C, Garcia-Pagán J-C *et al.* CO_2 wedged hepatic venography in the evaluation of portal hypertension. *Gut* 2000; **46**: 856–60.
9 Futagawa S, Fukazawa M, Musha H *et al.* Hepatic venography in noncirrhotic idiopathic portal hypertension. *Radiology* 1981; **141**: 303–9.
10 Scott J, Dick R, Long RG *et al.* Percutaneous transhepatic obliteration of gastro-oesophageal varices. *Lancet* 1976; **2**: 53–5.
11 Futagawa S, Fukazawa M, Horisawa M *et al.* Portographic liver changes in idiopathic noncirrhotic portal hypertension. *AJR Am. J. Roentgenol.* 1980; **134**: 917–23.
12 Kimura K, Tsuchiya Y, Ohto M *et al.* Single-puncture method for percutaneous transhepatic portography using a thin needle. *Radiology* 1981; **139**: 748–9.
13 Funaki B, Rosenblum JD, Leef JA *et al.* Percutaneous treatment of portal venous stenosis in children and adolescents with segmental hepatic transplants: long-term results. *Radiology* 2000; **215**: 147–51.
14 Stein M, Schneider PD, Ho HS, Eckert R, Urayama S, Bold RJ. Percutaneous transhepatic portography with intravascular ultrasonography for evaluation of venous involvement of hepatobiliary and pancreatic tumors. *J. Vasc. Interv. Radiol.* 2002; **13**: 805–14.
15 The Japan Society for Portal Hypertension. *The General Rules for Study of Portal Hypertension*, 2nd edn., 2004; 91–2.
16 Cho DR, Cho KJ, Hawkins IF Jr. Potential air contamination during CO_2 angiography using a hand-held syringe: theoretical considerations and gas chromatography. *Cardiovasc. Intervent. Radiol.* 2006; **29**: 637–41.
17 Kimura K, Ohto M, Matsutani S, Furuse J, Hoshino K, Okuda K. Relative frequencies of portosystemic pathways and renal shunt formation through the "posterior" gastric vein: portographic study in 460 patients. *Hepatology* 1990; **12**: 725–8.
18 Watanabe K, Kimura K, Matsutani S *et al.* Portal hemodynamics in patients with gastric varices: a study in 230 patients with esophageal and/or gastric varices using portal vein catheterization. *Gastroenterology* 1988; **95**: 434–40.
19 von Herbay A, Frieling T, Haeussinger D. Color Doppler sonographic evaluation of spontaneous portosystemic shunts and

inversion of portal venous flow in patients with cirrhosis. *J. Clin. Ultrasound* 2000; **28**: 332–9.
20 Anderson CM. GI magnetic resonance angiography. *Gastrointest. Endosc.* 2002; **55**: S42–8.
21 Taourel P, Blanc P, Dauzat M *et al.* Doppler Study of mesenteric, hepatic, and portal circulation in alcoholic cirrhosis: relationship between quantitative Doppler measurements and the severity of portal hypertension and hepatic failure. *Hepatology* 1998; **28**: 932–6.
22 Lin J, Zhou KR, Chen ZW, Wang JH, Yan ZP, Wang YX. 3D contrast-enhanced MR portography and direct X-ray portography: a correlation study. *Eur. Radiol.* 2003; **13**: 1277–85.
23 Madoff DC, Abdalla EK, Vauthey JN. Portal vein embolization in preparation for major hepatic resection: evolution of a new standard of care. *J. Vasc. Interv. Radiol.* 2005; **16**: 779–90.
24 Abulkhir A, Limonqelli P, Healey AJ *et al.* Preoperative portal vein embolization for major liver resection: a meta-analysis. *Ann. Surg.* 2008; **247**: 49–57.
25 Adani GL, Baccarani U, Risaliti A *et al.* Percutaneous transhepatic portography for the treatment of early portal vein thrombosis after surgery. *Cardiovasc. Intervent. Radiol.* 2007; **30**: 1222–6.
26 Shibata T, Itoh K, Kubo T *et al.* Percutaneous transhepatic balloon dilation of portal venous stenosis in patients with living donor liver transplantation. *Radiology* 2005; **235**: 1078–83.
27 Mizumoto H, Matsutani S, Fukuzawa T *et al.* Hemodynamics in the left gastric vein after endoscopic ligation of esophageal varices combined with sclerotherapy. *J. Gastroenterol. Hepatol.* 2001; **16**: 495–500.

Research Article

EASL EUROPEAN ASSOCIATION FOR THE STUDY OF THE LIVER | JOURNAL OF HEPATOLOGY

The polycomb group gene product Ezh2 regulates proliferation and differentiation of murine hepatic stem/progenitor cells

Ryutaro Aoki[1,2,†], Tetsuhiro Chiba[1,2,3,†], Satoru Miyagi[1], Masamitsu Negishi[1], Takaaki Konuma[1], Hideki Taniguchi[4], Makoto Ogawa[2], Osamu Yokosuka[2], Atsushi Iwama[1,3,*]

[1]*Department of Cellular and Molecular Medicine, Graduate School of Medicine, Chiba University, 1-8-1 Inohana, Chuo-ku, Chiba 260-8670, Japan;* [2]*Department of Medicine and Clinical Oncology, Graduate School of Medicine, Chiba University, 1-8-1 Inohana, Chuo-ku, Chiba 260-8670, Japan;* [3]*JST, CREST, Sanbancho, Chiyoda-ku, Tokyo 102-0075, Japan;* [4]*Department of Regenerative Medicine, Graduate School of Medicine, Yokohama City University, 3-9 Fukuura, Kanazawa-ku, Kanagawa 236-0004, Japan*

Background & Aims: Polycomb group proteins initiate and maintain gene silencing through chromatin modifications and contribute to the maintenance of self-renewal in a variety of stem cells. Among polycomb repressive complexes (PRCs), PRC2 initiates gene silencing by methylating histone H3 lysine 27, and PRC1 maintains gene silencing through mono-ubiquitination of histone H2A lysine 119. We have previously shown that Bmi1, a core component of PRC1, tightly regulates the self-renewal of hepatic stem/progenitor cells.

Methods: In this study, we conducted lentivirus-mediated knockdown of *Ezh2* to characterise the function of Ezh2, a major component of PRC2, in hepatic stem/progenitor cells.

Results: Loss of *Ezh2* function in embryonic murine hepatic stem/progenitor cells severely impaired proliferation and self-renewal capability. This effect was more prominent than that of *Bmi1*-knockdown and was partially abrogated by the deletion of both *Ink4a* and *Arf*, major targets of PRC1 and PRC2. Importantly, *Ezh2*-knockdown but not *Bmi1*-knockdown promoted the differentiation and terminal maturation of hepatocytes, followed by the up-regulation of several transcriptional regulators of hepatocyte differentiation.

Conclusions: Our findings indicate that Ezh2 plays an essential role in the maintenance of both the proliferative and self-renewal capacity of hepatic stem/progenitor cells and the full execution of their differentiation.

Keywords: Hepatic stem/progenitor cells; Ezh2; Bmi1; Ink4a/Arf; Self-renewal; Differentiation.

Received 18 September 2009; received in revised form 12 January 2010; accepted 14 January 2010; available online 24 March 2010

* Corresponding author. Address: Department of Cellular and Molecular Medicine, Graduate School of Medicine, Chiba University, 1-8-1 Inohana, Chuo-ku, Chiba 260-8670, Japan. Tel.: +81 43 2262187; fax: +81 43 2262191.

E-mail address: aiwama@faculty.chiba-u.jp (A. Iwama).

† These authors contributed equally to this work.

Abbreviations: PcG, polycomb group; PRC, polycomb repressive complex; H3K27, histone H3 at lysine 27; HCC, hepatocellular carcinoma; ED, embryonic day; EHS, Engelbreth–Holm–Swarm; OSM, oncostatin M; TNF, tumour necrosis factor; shRNA, short-hairpin RNA; ERP, enhanced red fluorescence protein; ChIP, chromatin immunoprecipitation; EGFP, enhanced green fluorescence protein; Alb, albumin; CK, cytokeratin; Epcam, epithelial cell adhesion molecule; ELISA, enzyme-linked immunosorbent assay; Gata1, GATA binding protein 1; TAT, tyrosine aminotransferase; G6P, glucose-6-phosphatase; PAS, periodic acid-Schiff; Itgb, integrin β; ES, embryonic stem; Hnf, hepatocyte nuclear factor; Cebp, CCAAT/enhancer binding protein.

Introduction

Stem cells are generally defined as self-renewing cell populations that can differentiate into multiple distinct cell types. Liver has an enormous capacity to regenerate after injury, although the mechanism of hepatic regeneration differs depending on the proliferation of pre-existing hepatocytes, homing of bone marrow cells, and proliferation and differentiation of hepatic stem cells [1]. In the developing murine liver, endodermal-derived hepatoblasts or hepatic stem/progenitor cells differentiate into hepatocytes and cholangiocytes [1]. Although hepatic stem/progenitor cells have been successfully identified in murine foetal liver [2,3], the molecular pathways regulating the self-renewal and differentiation of these cells are poorly understood.

Polycomb group (PcG) proteins form multiprotein complexes that play important roles in maintaining the transcriptional repression of target genes. Although PcG genes are best known for their role in maintaining the repression of *Hox* genes during development, they have been implicated in stem cell self-renewal and differentiation [4]. The PcG gene family members form two major distinct PcG complexes: one complex, known as polycomb repressive complex (PRC) 1, is composed of Ring1a/1b, Mph1, and Bmi1 or Mel18, and the other complex, PRC2, is composed of Eed, Suz12, and Ezh2. Ezh2 is a PcG protein homologous to *Drosophila* enhancer of zeste, a histone methyltransferase associated with transcriptional repression. Ezh2 has a SET domain that is typical of histone methyltransferases, and it catalyses the addition of methyl groups to histone H3 at lysine 27 (H3K27). In many cases, the methylation of H3K27 by Ezh2 results in the recruitment of PRC1, and the two PRCs cooperate in gene silencing [4]. Notably, expression of EZH2 together with BMI1 is reportedly associated with the progression and aggressiveness of hepatocellular carcinoma (HCC), and *EZH2*-knockdown inhibits the growth of cul-

tured human HCC cell lines [5]. We previously reported that Bmi1 enhances the self-renewal capacity of hepatic stem/progenitor cells and drives cancer initiation [6]. However, the role of Ezh2 in the hepatic stem cell system remains to be clarified.

In this study, we investigated the function of Ezh2 in foetal liver Dlk$^+$ hepatic stem/progenitor cells by knocking down *Ezh2* using lentivirus-mediated stable shRNA expression. *Ezh2*-knockdown profoundly inhibited the proliferation of Dlk$^+$ hepatic stem/progenitor cells and promoted differentiation into hepatocytes. These findings provide the first evidence of an essential role for Ezh2 in the homeostasis of the hepatic stem cell system.

Materials and methods

Mice

Pregnant C57BL/6 mice were purchased from Japan SLC (Hamamatsu, Japan). *Ink4a–Arf*$^{+/-}$ mice (Strain code 01XB1) obtained from Mouse Models of Human Cancers Consortium in NCI-Frederick (Frederick, MD, USA) were bred and maintained in accordance with our institutional guidelines for the use of laboratory animals.

Purification and culture of Dlk$^+$ cells

Dlk$^+$ cells were prepared from liver cell suspensions of embryonic day (ED) 14.5 foetal livers as described previously [2,3]. Briefly, cells were stained with rat anti-mouse Dlk monoclonal antibody (MBL, Nagoya, Japan) followed by anti-rat IgG-conjugated magnetic beads. Dlk$^+$ cells were purified by passage through cell separation columns in a magnetic field (Miltenyi Biotec, Bergisch Gladbach, Germany). They were plated at 1×10^3 cells/well on collagen type IV-coated 6-well plates (Becton Dickinson, Franklin lakes, NJ, USA) and cultured as described elsewhere [2,3]. Colony assays were performed in at least three independent triplicate experiments. To evaluate the potential to differentiate into hepatocytes, Dlk$^+$ cells were placed on an Engelbreth–Holm–Swarm (EHS) gel (Becton–Dickinson) in the presence of oncostatin M (OSM, R&D Systems, Minneapolis, MN, USA) [7]. Collagen type I gel culture (Nitta Gelatin, Osaka, Japan) in the presence of tumour necrosis factor (TNF)-α (Peprotech, Rocky Hill, NJ, USA) was also conducted to examine the ability to differentiate into cholangiocytes [8].

Viral production and transduction

Lentiviral vectors (CS-H1-shRNA-EF-1α-EGFP) expressing short-hairpin RNAs (shRNAs) against murine *Ezh2* (target sequence: sh-*Ezh2*-1, 5′-GGAAAGAACTGAAACCTTA-3′; sh-*Ezh2*-2, 5′-GGTAAATGCTCTTGGTCAA-3′) were constructed. Lentiviral vectors (CS-H1-shRNA-EF-1α-EGFP) expressing shRNAs against *Bmi1* and *luciferase* were also used [6]. A lentiviral vector carrying enhanced red fluorescent protein (ERP) (CS-H1-shRNA-RfA-ERP) expressing shRNA against *Bmi1* was also constructed for the double knockdown of *Ezh2* and *Bmi1*. Recombinant lentiviruses were produced as described previously [6]. Purified cells were transduced with indicated viruses 12–18 h after pre-incubation.

Chromatin immunoprecipitation

Chromatin immunoprecipitation (ChIP) was performed as reported previously [9]. Briefly, cross-linked chromatin was sonicated into 200- to 500-bp fragments. The chromatin was immunoprecipitated using anti-Ezh2 (clone AC22, a gift from Dr. Kristian Helin) and anti-H3K27me3 (Millipore, Bedford, MA, USA) antibodies. Normal mouse IgG was used as a negative control. Quantitative PCR was conducted using SYBR Premix Ex Taq II (Takara Bio, Otsu, Japan). Primer sequences are listed in Supplementary Table 1 [10].

Statistics

Data are presented as the means ± SEM. Statistical differences were analysed using the Mann–Whitney *U* test. *p* values less than 0.05 were considered significant.

Results

Basal expression of Ezh2 and stable knockdown of Ezh2 in hepatic stem/progenitor cells

We first analysed the mRNA expression of *Ezh2* in hepatic stem/progenitor cells, which are enriched in the Dlk$^+$ cell fraction [2,3] in ED14.5 foetal liver. Haematopoietic cells were excluded by gating the CD45$^-$Ter119$^-$ cell fraction, and liver cells were divided into the Dlk$^+$ hepatic stem/progenitor fraction and the Dlk$^-$ non-stem/progenitor fraction. *Ezh2* expression was readily detected in both fractions, but quantitative RT-PCR and western blot analyses revealed a higher level of *Ezh2* expression in the Dlk$^+$ than the Dlk$^-$ fraction (Fig. 1A and B).

To investigate the function of Ezh2 in Dlk$^+$ hepatic stem/progenitor cells, we used lentivirus-mediated *Ezh2*-knockdown. Dlk$^+$ cells prepared from ED14.5 wild-type foetal livers were infected with sh-*Ezh2* viruses and allowed to propagate for 5 days. Flow-cytometric analyses revealed that the majority (more than 90%) of cells were positive for enhanced green fluorescent protein (EGFP), a marker of lentiviral integration (Fig. 1C). We compared the effect of the two shRNAs against *Ezh2* (sh-*Ezh2*-1 and sh-*Ezh2*-2) by real-time RT-PCR and western blot analyses. Real-time RT-PCR showed that the level of endogenous Ezh2 was markedly reduced in cells infected with lentivirus expressing shRNA against *Ezh2* compared with the control cells expressing shRNA against *luciferase* (sh-*Luc*) at multiple time points (Fig. 1D). Both shRNA severely reduced Ezh2 expression, although sh-*Ezh2*-2 was less effective than sh-*Ezh2*-1 (Fig. 1D). Concordant with this, the western blot analysis of cells at day 5 of culture showed that sh-*Ezh2*-1 was more effective in knocking down *Ezh2* than sh-*Ezh2*-2 (Fig. 1E). Therefore, we mainly used sh-*Ezh2*-1 in the following experiments, but we also obtained very similar results with sh-*Ezh2*-2 (Fig. 2C, D and data not shown).

Impaired proliferation and self-renewal of Dlk$^+$ cells following Ezh2-knockdown

It has been reported that approximately 15% of purified Dlk$^+$ cells gave rise to colonies at day 5 of culture. Among them, Dlk$^+$ cells, with the ability to form large colonies consisting of more than 100 cells at day 5 of culture, possess the properties of hepatic stem/progenitor cells. Because Dlk$^+$ cells produce a large number of Dlk$^-$ progeny, the proportion of Dlk$^+$ cells declines to less than 1% at day 5 of culture. Nonetheless, Dlk$^+$ cells in culture retain clonogenic activity [2,3]. Corresponding to these reports, almost 15% of Dlk$^+$ cells gave rise to colonies, which included a significant number of large colonies, while Dlk$^-$ cells scarcely gave rise to colonies, and no Dlk$^-$ cells generated large colonies at day 5 of culture (Fig. 2A). Next, we performed loss-of-function assays of *Ezh2* and/or *Bmi1* in Dlk$^+$ cells. Knockdown efficiencies were confirmed by western blot (Figs. 1E and 2B). *Ezh2*-knockdown modestly decreased the total number of colonies formed at day 5 of culture (Fig. 2C). By contrast, the number of large colonies derived from *Ezh2*-knockdown Dlk$^+$ cells was significantly decreased compared with the control, and most of the *Ezh2*-knockdown cells did not proliferate beyond 14 days (Fig. 2D). The effect of *Bmi1*-knockdown was milder than that of *Ezh2*-knockdown, and double knockdown of *Ezh2* and *Bmi1* had a limited advantage over single knockdown of *Ezh2* in inhibiting the proliferation of Dlk$^+$ cells

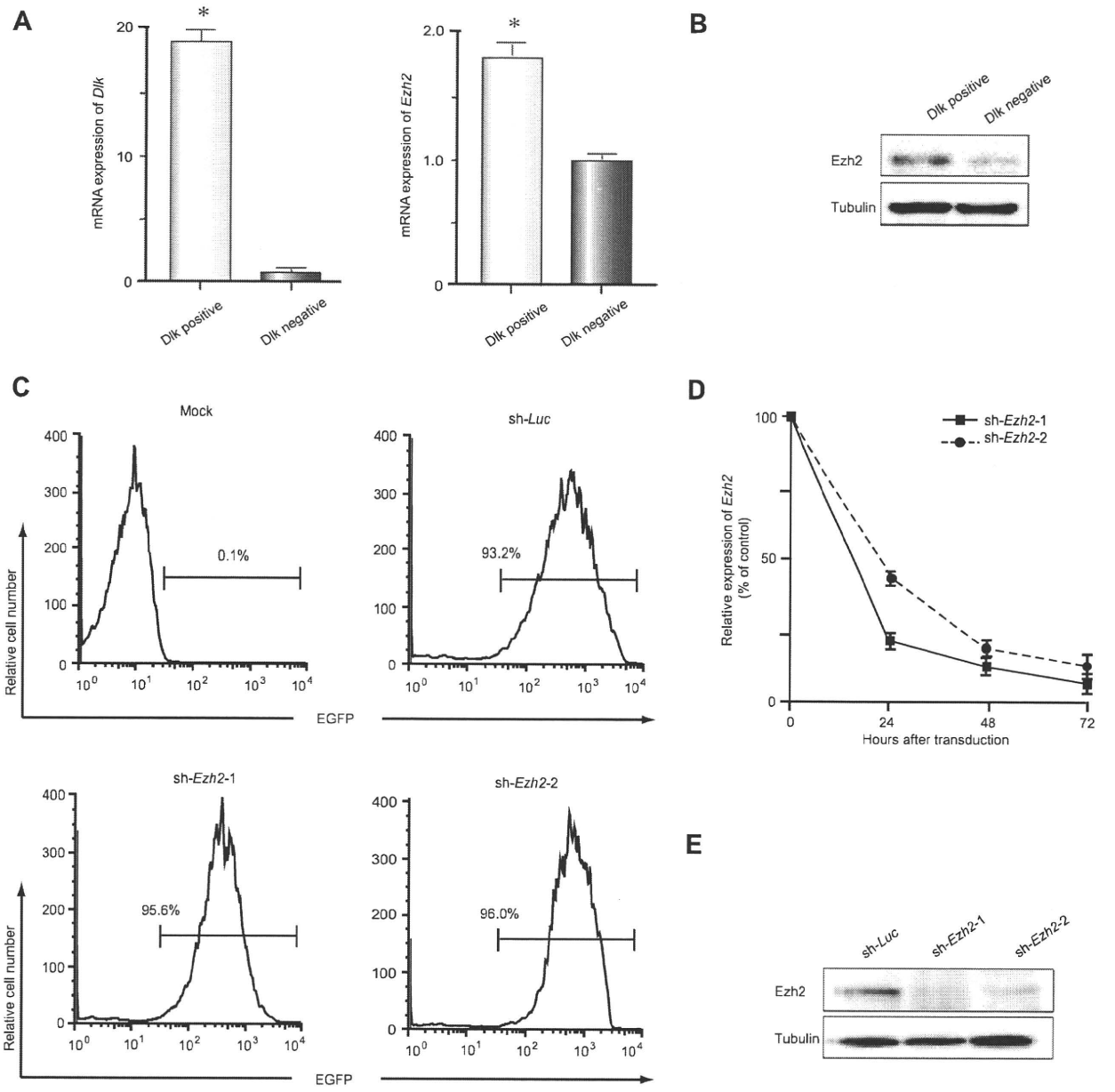

Fig. 1. Basal expression of *Ezh2* in wild-type and *Ezh2*-knockdown hepatic stem/progenitor cells. (A) Real-time RT-PCR analysis of *Dlk* and *Ezh2* expression in freshly purified Dlk$^+$ cells. *Statistically significant (p <0.05). (B) Western blot analysis of Ezh2 expression in freshly purified Dlk$^+$ cells compared to Dlk$^-$ cells. (C) The EGFP-positivity of cells transduced with indicated viruses. (D) Real-time RT-PCR analysis of *Ezh2* expression in Dlk$^+$ cells transduced with sh-*Ezh2*-1 or sh-*Ezh2*-2. A lentiviral vector expressing shRNA against *luciferase* (sh-*Luc*) was used as a control. Expression relative to the control is depicted. (E) Dlk$^+$ cells transduced with sh-*Ezh2*-1 or sh-*Ezh2*-2 were subjected to western blot analysis at day 5 of culture.

(Fig. 2C and D). Although *Ezh2*-knockdown enhanced apoptotic cell death in cultures of Dlk$^+$ cells, levels of apoptosis were not prominent in control or *Ezh2*-knockdown cultures (1.1 ± 0.2 and 3.6 ± 0.5%, respectively, Fig. 2E).

Among the colonies derived from hepatic stem/progenitor cells, those that keep growing beyond 28 days retain a significant number of hepatic stem/progenitor cells and efficiently generate secondary colonies in replating assays [6]. Because it is difficult to culture *Ezh2*-knockdown Dlk$^+$ cells beyond 14 days, we recovered cells from uninfected colonies that kept growing beyond 28 days and infected them with sh-*Ezh2* viruses. At day 7 of culture, Dlk$^+$EGFP$^+$ cells expressing sh-*Ezh2*-1 were collected by cell sorting and replated in order to allow the formation of colonies. The frequencies of total secondary colonies and large secondary colonies were markedly reduced by *Ezh2*-knockdown compared to the control (Fig. 2F). Again, the inhibitory effect of *Ezh2*-knock-

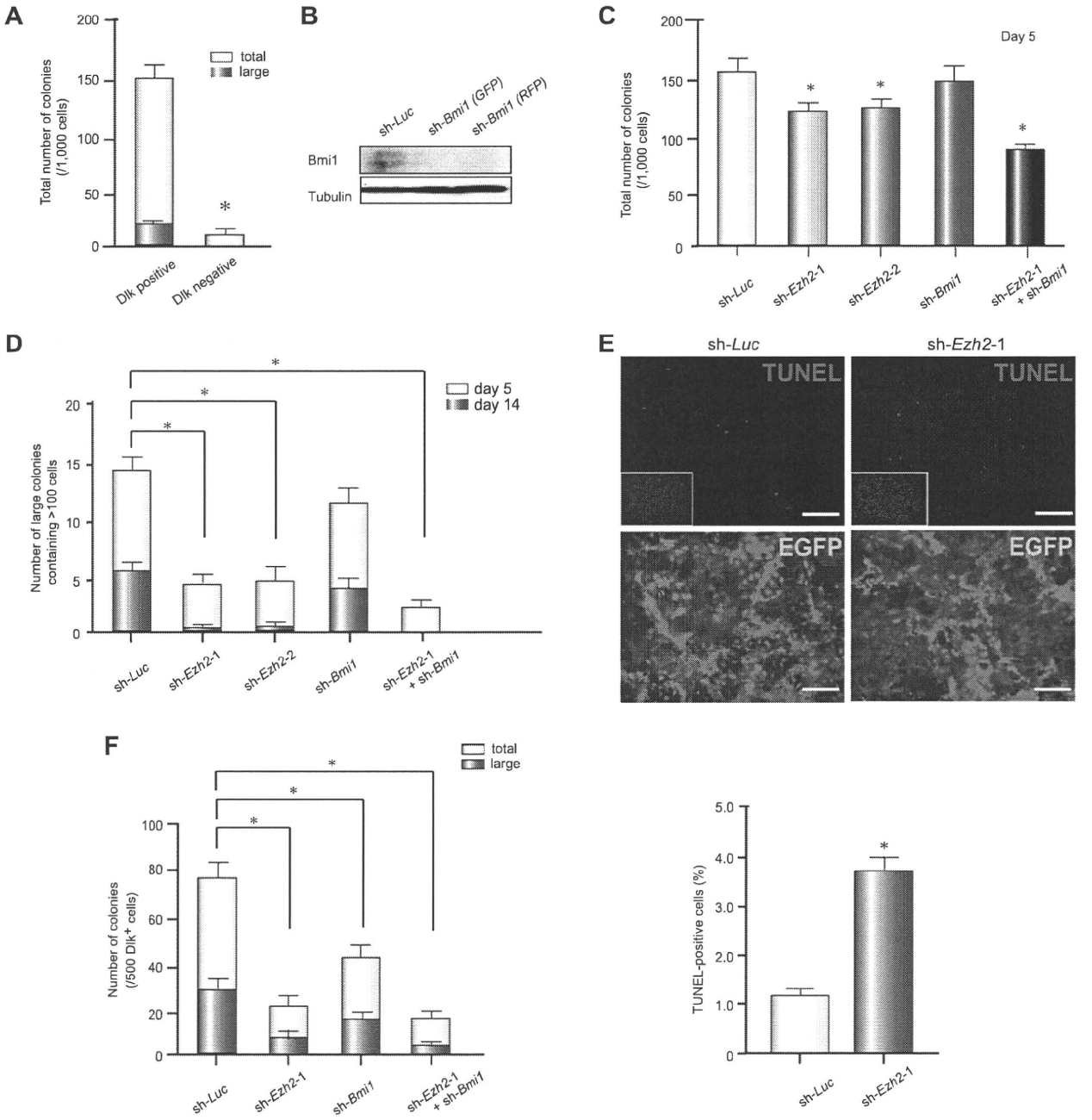

Fig. 2. Loss-of-function analyses of *Bmi1* and *Ezh2* on hepatic stem/progenitor cell proliferation. (A) The number of total colonies and large colonies consisting of more than 100 cells generated from 1000 Dlk^+ or Dlk^- cells was counted at day 5 of culture. *Statistically significant ($p < 0.05$) (B) Dlk^+ cells expressing shRNA against *Bmi1* together with *EGFP* or *RFP* as a marker gene were subjected to western blot analysis at day 5 of culture. (C) Numbers of colonies generated from 1000 Dlk^+ cells transduced with indicated viruses. Total numbers of colonies were counted at day 5 of culture. *Statistically significant ($p < 0.05$) (D) The number of large colonies containing more than 100 cells at days 5 and 14. *Statistically significant ($p < 0.05$). (E) TUNEL assays (upper panels) and fluorescence images (lower panels) of colonies at day 5 of culture. Nuclear DAPI staining (blue) is shown in the insets (upper panels). *Statistically significant ($p < 0.05$). Scale bar = 500 μm. (F) Effect of *Ezh2*-knockdown on replating capacity. Among the colonies derived from uninfected Dlk^+ cells, those which kept growing beyond 28 days were infected with viruses expressing shRNAs. Seven days after infection, Dlk^+EGFP^+ cells were collected by cell sorting and replated to allow colonies to form. The total number of total colonies and large colonies consisting of more than 100 cells were counted at day 7 of subculture. *Statistically significant ($p < 0.05$).

down was greater than that of *Bmi1*-knockdown, and double knockdown minimally enhanced the inhibitory effect of *Ezh2*-knockdown. These results suggest that Ezh2 plays an essential role in the maintenance of both the proliferative and self-renewal capacity in hepatic stem/progenitor cells. Colony PCR demonstrated that secondary large colonies expressed both hepatocyte

markers and cholangiocyte markers (Supplementary Fig. 1), indicating that the ability to differentiate into either hepatocytes or cholangiocytes was maintained in replated Dlk$^+$ cells. Of interest, the *Ezh2*-knockdown colonies showed a higher expression level of *albumin* (*Alb*) than the control colonies, whereas *Bmi1*-knockdown caused a mild increase in the expression of *Sall4*, which is a regulator of cholangiocyte differentiation [11].

Role of Ezh2 in differentiation of hepatic stem/progenitor cells

Ezh2 has recently been implicated in the differentiation of neural stem cells and epidermal stem cells [12,13]. However, its role in hepatic stem/progenitor cells remains to be addressed. In the control colonies, cytokeratin (CK) 7$^+$ cholangiocytes predominantly differentiated compared to Alb$^+$ hepatocytes. By contrast, comparable numbers of Alb$^+$ hepatocytes were detected in the colonies generated from *Ezh2*-knockdown Dlk$^+$ cells (Fig. 3A and B). Although *Bmi1*-knockdown did not significantly compromise the differentiation of Dlk$^+$ cells, double-knockdown colonies contained an increased number of Alb$^+$ hepatocytes as in *Ezh2*-knockdown (Fig. 3A and B). These results suggest that *Ezh2*-knockdown promotes the differentiation of hepatic stem/progenitor cells towards the hepatocyte lineage. Consistent with this finding, an enzyme-linked immunosorbent assay (ELISA) detected a significant increase in Alb secretion from culture of *Ezh2*-knockdown Dlk$^+$ cells compared to that of control Dlk$^+$ cells (Supplementary Fig. 2A). The expression of liver-enriched transcription factors was up-regulated in both *Ezh2*- and *Bmi1*-knockdown Dlk$^+$ cells at day 5 of culture (Fig. 3C). However, the increase was mild in the *Bmi1*-knockdown Dlk$^+$ cells compared to the *Ezh2*-knockdown or double-knockdown cells. A slight increase in the expression of *Sall4* was also observed in *Bmi1*-knockdown and double-knockdown cells. In clear contrast, neither *Ezh2*- nor *Bmi1*-knockdown Dlk$^+$ cells showed remarkable changes in the expression of *Gata1* (*GATA binding protein 1*), a haematopoietic transcription factor gene (Fig. 3C).

Regulation of the Ink4a/Arf gene by Ezh2

Bmi1, a core component of PRC1, regulates the self-renewal of various somatic stem cells, targeting $p16^{Ink4a}$ and $p19^{Arf}$ in particular [14,15]. Ezh2 likewise contributes to the repression of the *Ink4a/Arf* locus in mouse embryonic fibroblasts [16].

To examine whether *Ezh2*-knockdown results in derepression of the *Ink4a* and *Arf* genes, we performed real-time RT-PCR analyses. Expression of both $p16^{Ink4a}$ and $p19^{Arf}$ was up-regulated in *Ezh2*-knockdown Dlk$^+$ cells at day 5 of culture, although their derepression levels were moderate compared with those in *Bmi1*-knockdown cells (Fig. 4A). To address whether Ezh2 is involved in transcriptional repression through histone modifications at the *Ink4a/Arf* locus, we conducted ChIP analyses in wild-type Dlk$^+$ cells. ChIP assays demonstrated the binding of Ezh2 across the *Ink4a/Arf* locus and an increase in H3K27me3 levels (Fig. 4B).

Loss-of-function assays of Ezh2 in Ink4a/Arf$^{-/-}$ Dlk$^+$ cells

To evaluate directly the involvement of the *Ink4a/Arf* locus in Ezh2 function in hepatic stem/progenitor cells, we isolated Dlk$^+$ cells from *Ink4a–Arf$^{-/-}$* embryos. Deletion of the *Ink4a/Arf* locus significantly enhanced the propagation of colonies compared to the wild-type Dlk$^+$ cells, and most of the colonies at day 5 of culture kept expanding up to day 14 (Fig. 5A and B). Flow-cytometric analysis at day 14 of culture revealed that the percentage of Dlk$^+$ cells in *Ink4a/Arf$^{-/-}$* colonies was approximately 9-fold higher than in wild-type colonies (data not shown), indicating that deletion of the *Ink4a/Arf* locus enhanced the self-renewal capability of Dlk$^+$ cells. Notably, however, not only the total number of colonies but also the number of large colonies (consisting of more than 100 cells at day 5 of culture) was significantly reduced by *Ezh2*-knockdown (Fig. 5A and B). Consistent with this, the diameter of large *Ezh2*-knockdown colonies at day 14 of culture was significantly smaller than in the control (Fig. 5C). Of interest, the effect of *Bmi1*-knockdown was largely cancelled by the deletion of *Ink4a/Arf*, while that of *Ezh2*-knockdown was only partially abrogated (Fig. 5A–C). Immunostaining revealed that large colonies derived from *Ezh2*-knockdown *Ink4a-Arf$^{-/-}$*Dlk$^+$ cells still harboured a similar number of Alb$^+$ hepatocytes as those derived from *Ezh2*-knockdown wild-type Dlk$^+$ cells (Fig. 5D and E).

We next performed replating assays. At day 14 of culture, *Ink4a-Arf$^{-/-}$*Dlk$^+$EGFP$^+$ cells transduced with knockdown vectors were collected by cell sorting and replated to allow colonies to form. The frequency of total secondary colonies and of large secondary colonies was markedly reduced by *Ezh2*-knockdown compared to the control (Supplementary Fig. 3A). Deletion of the *Ink4a/Arf* locus cancelled out the effect of *Ezh2*-knockdown to a lesser extent than that of *Bmi1*-knockdown. Secondary colonies were generated in a similar fashion to the original colonies and exhibited enhanced differentiation towards the hepatocyte lineage (Supplementary Fig. 3B).

Role of Ezh2 in terminal differentiation and maturation in wild-type and Ink4a/Arf$^{-/-}$ Dlk$^+$ cells

We cultured Dlk$^+$ cells in EHS gel supplemented with OSM to selectively induce hepatocyte terminal maturation. By day 5 of culture, multiple cell clusters with tight cell–cell contact were formed. The *Ezh2*-knockdown clusters consisted of mature hepatocytes with a highly condensed, granulated cytosol and clear round nuclei compared with the control clusters (Fig. 6A). In addition, real-time RT-PCR revealed that tyrosine aminotransferase (*TAT*) and glucose-6-phosphatase (*G6P*), the metabolic enzyme genes highly expressed in terminally differentiated hepatocytes, were significantly up-regulated in *Ezh2*-knockdown cells (Fig. 6B). In addition, periodic acid-Schiff (PAS) staining successfully detected intracellular glycogen accumulation in *Ezh2*-knockdown cells, which indicated the functional maturation of the hepatocytes (Supplementary Fig. 2B). Although the deletion of *Ink4a/Arf* in Dlk$^+$ cells slightly promoted hepatocyte maturation in EHS gel cultures compared to wild-type Dlk$^+$ cells, *Ezh2*-knockdown further promoted hepatocyte maturation (Fig. 6A and B). Together, these findings indicate that post-commitment hepatocyte maturation is facilitated by *Ezh2*-knockdown.

Next, Dlk$^+$ cells were cultured on collagen type I gel in the presence of TNF-α to selectively induce differentiation into cholangiocytes. Both the control and *Ezh2*-knockdown cells similarly formed tube-like structures (Fig. 6C). Expression of *CK7*, *CK19* and integrin β4 (*Itgb4*), useful marker genes of cholangiocyte maturation, was mildly up-regulated in *Ezh2*-knockdown cells, but another marker gene, *Sall4*, did not show any changes in expression (Fig. 6D). The deletion of the *Ink4a/Arf* genes caused no

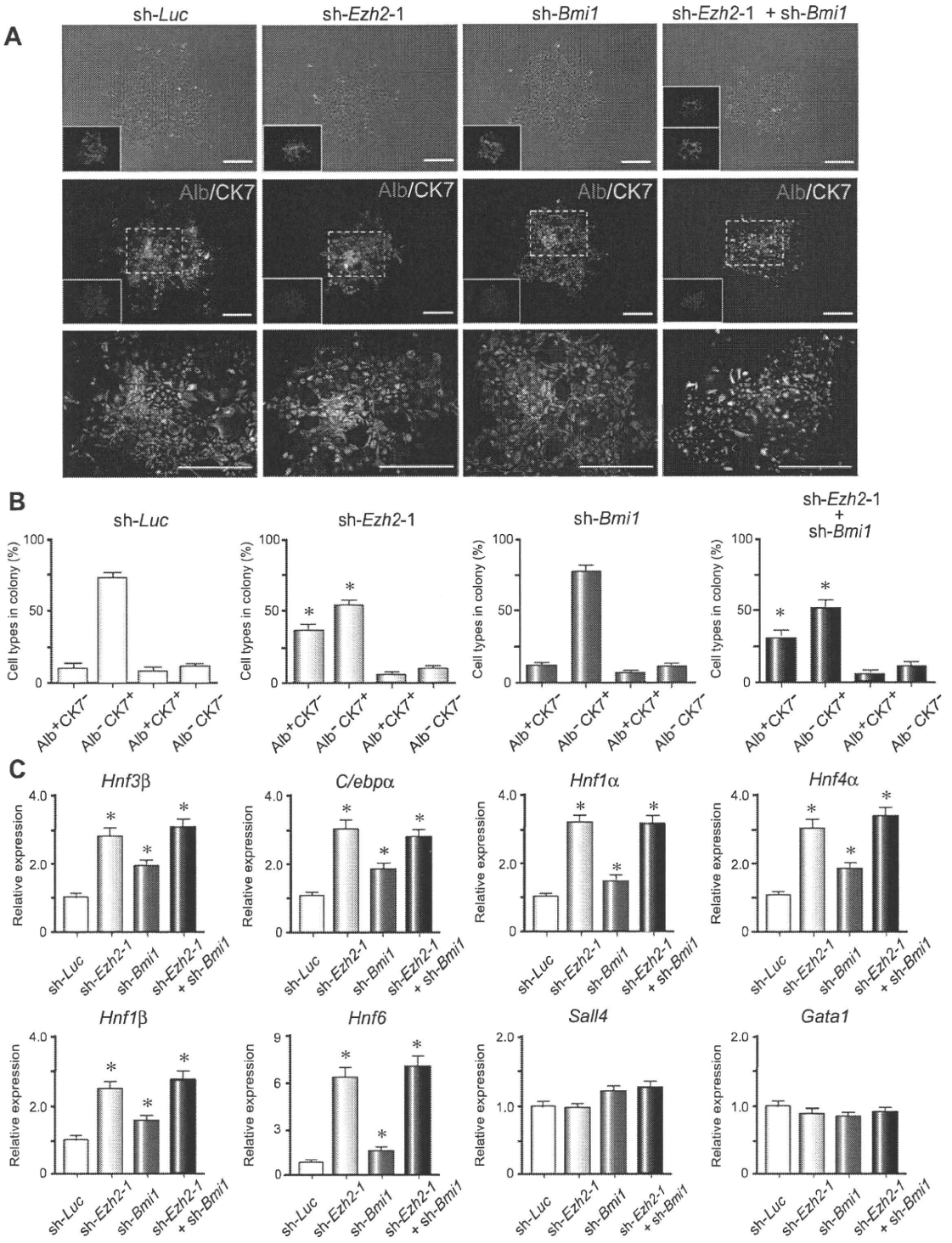

Fig. 3. Effects of *Ezh2*- and *Bmi1*-knockdown on the differentiation of hepatic stem/progenitor cells. (A) Bright-field images and fluorescence micrographs of large colonies (containing more than 100 cells) transduced with indicated viruses at day 5 of culture. Dual immunostaining was performed to detect the expression of Alb (red) and CK7 (green) in clonal colonies. EGFP expression in single-knockdown colonies, EGFP and RFP expression in a double-knockdown colony (upper panels) and nuclear DAPI staining (middle panels) are shown in the insets. Scale bar = 200 μm. (B) The percentages of Alb^+CK7^-, Alb^-CK7^+, Alb^+CK7^+, and Alb^-CK7^- cells in large colonies containing more than 100 cells were calculated at day 5 of culture. The average for 10 colonies is presented as the mean ± SD. *Statistically significant ($p < 0.05$). (C) Real-time RT-PCR analysis of the expression of liver-enriched transcription factors and *Gata1* in colonies derived from Dlk^+ cells transduced with indicated viruses at day 5 of culture. *Statistically significant ($p < 0.05$).

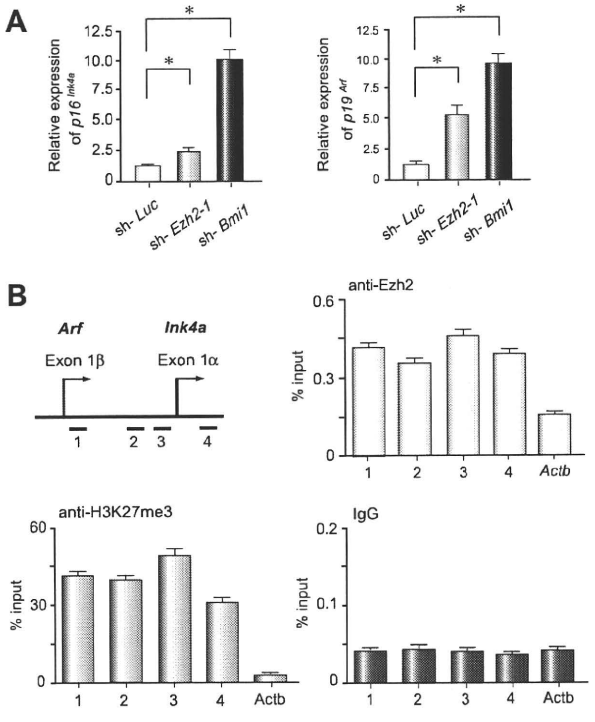

Fig. 4. Regulation of the *Ink4a/Arf* genes by Ezh2 in hepatic stem/progenitor cells. (A) Real-time RT-PCR analyses of $p16^{Ink4a}$ and $p19^{Arf}$ expression in colonies derived from Dlk$^+$ cells transduced with indicated viruses at day 5 of culture. *Statistically significant (p <0.05). (B) ChIP analyses of freshly purified Dlk$^+$ cells were conducted on the *Ink4a/Arf* locus (primer set 1–4) and the β-actin (*Actb*) control promoter region using indicated antibodies.

remarkable changes in collagen type I gel cultures in terms of cholangiocyte maturation (Fig. 6C and D).

Taken together, these findings indicate that post-commitment hepatocyte maturation rather than cholangiocyte maturation is accelerated by *Ezh2*-knockdown. Moreover, these results suggest that the *Ink4a/Arf* locus is also a major target of Ezh2, but there exist additional targets of Ezh2 in the regulation of hepatic stem/progenitor cell growth and self-renewal.

Discussion

Ezh2 plays an important role in gene silencing through the trimethylation of H3K27. In embryonic stem (ES) cells, most developmental genes are reversibly silenced through the bivalent domain in their transcriptional regulatory region, which consists of large regions of trimethylated H3K27 harbouring smaller regions of trimethylated H3K4 [17,18]. Therefore, PRC2 is critical in maintaining the pluripotency of embryonic stem (ES) cells. However, little is known about the role of PRC2 in somatic stem cells, especially in primary hepatic stem/progenitor cells. Our loss-of-function analysis of *Ezh2* clearly showed that Ezh2 regulates the proliferation of hepatic stem/progenitor cells in *Ink4a/Arf*-dependent and -independent manners. Given that *Ezh2*-knockdown profoundly affected the replating efficiency of hepatic stem/progenitor cells, Ezh2 might also be needed to maintain the self-renewal capacity of these cells. These functional characteristics of Ezh2 are very similar to those of Bmi1, but Ezh2 behaved quite differently from Bmi1 in the regulation of hepatic stem/progenitor cell differentiation. *Ezh2*-knockdown promoted the differentiation of hepatic stem/progenitor cells into hepatocytes and further enhanced the maturation of hepatocytes. However, *Bmi1*-knockdown did not compromise their differentiation. These findings unveil distinct functions of PRC1 and PRC2 in the regulation of hepatic stem/progenitor cell differentiation. A similar finding has been reported in breast cancer, in which EZH2 and BMI1 inversely correlate with prognosis and TP53 mutation [19].

Ink4a and *Arf* are major target genes of PcG proteins such as Bmi1 and Ezh2 [16]. Ezh2 contributes to the proliferation of pancreatic β-cells during regeneration by suppressing the *Ink4a/Arf* locus [20]. Overexpression of Ezh2 reportedly decreases expression of p16^{INK4a} through hypermethylation of the $p16^{INK4a}$ promoter in cholangiocarcinogenesis in hepatolithiasis [21]. The present ChIP analyses showed that Ezh2 binds to the *Ink4a/Arf* locus, accompanied by increased levels of trimethylated H3K27 in hepatic stem/progenitor cells. However, deletion of the *Ink4a/Arf* locus only partially abrogated the inhibitory effect of *Ezh2*-knockdown on the expansion of hepatic stem/progenitor cells. On the other hand, the inhibitory effect of *Bmi1*-knockdown was largely cancelled by deletion of *Ink4a/Arf*. These results indicate that Ezh2 regulates hepatic stem/progenitor cells in both *Ink4a/Arf*-dependent and -independent manners. Actually, double knockdown of *Ezh2* and *Bmi1* had a limited advantage over single knockdown of *Ezh2* in inhibiting hepatic stem/progenitor cell proliferation, further indicating additional functions of Ezh2 independent of Ink4a/Arf.

A number of liver-enriched transcription factors, including hepatocyte nuclear factors (Hnfs) and CCAAT/enhancer binding proteins (Cebps), play a central role in normal hepatogenesis [22]. It has been reported that Hnf3β, a marker of definitive endoderm, is indispensable for early liver development [23]. Consistent with this, enforced expression of Hnf3β in ES cells and mesenchymal stem cells promotes differentiation towards the hepatocyte lineage [24,25]. Recent studies have shown that Cebpα, a nuclear transcription factor of the bZIP protein family, is essential for hepatocyte differentiation [26]. In addition, suppression of Cebpα expression stimulates biliary cell differentiation, with reduced expression of Hnf6 and Hnf1β [27].

In the present study, *Ezh2*-knockdown in hepatic stem/progenitor cells resulted in enhanced expression of Hnfs. Likewise, increased expression of *Hnf6* and *Hnf1b* was simultaneously observed. Of interest, chromatin immunoprecipitation combined with DNA microarray (ChIP-on-chip) analyses reveal that both PRC1 and PRC2 can bind to the promoter regions of *Hnf3b*, *Cebpa*, and *Hnf6* in ES cells [28]. As *Hnf3b* and *Cebpa* have bivalent domains in their promoter regions [17,18], we hypothesised that *Ezh2* mediates the silencing of these genes to maintain hepatic stem/progenitor cells in an immature state. Unexpectedly, the present ChIP analyses using purified Dlk$^+$ cells failed to demonstrate the binding of Ezh2 at these loci (data not shown). It is possible that the Dlk$^+$ fraction was inappropriate for detecting the recruitment of Ezh2 for repression of target genes because it contained not only stem/progenitor cells but also cells in different stages of differentiation. Intriguingly, a recent study showed that Ezh2-dependent trimethylated H3K27 prevents the recruitment of AP1 and other transcription factors required for terminal differentiation [13]. It is also possible that Ezh2-dependent H3K27me3 on hepatocyte differentiation-related genes likewise

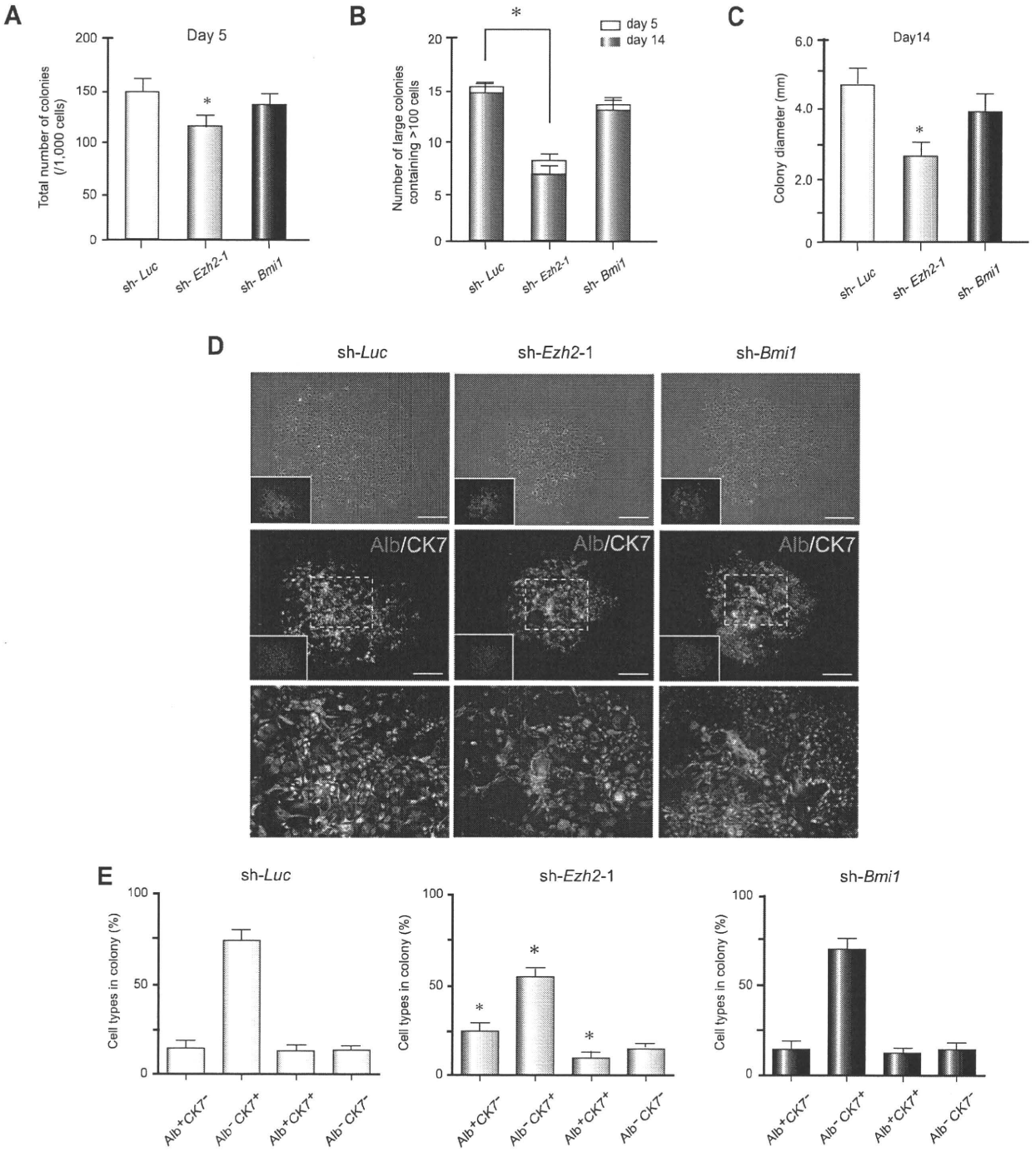

Fig. 5. Loss-of-function analyses of *Bmi1* and *Ezh2* on the proliferation of *Ink4a-Arf*$^{-/-}$ hepatic stem/progenitor cells. (A) Numbers of colonies generated from 1000 *Ink4a-Arf*$^{-/-}$Dlk^{+} cells transduced with indicated viruses. Total numbers of colonies were counted at day 5 of culture. *Statistically significant (p <0.05) (B) The number of large colonies containing more than 100 cells at days 5 and 14. *Statistically significant (p <0.05). (C) The diameter of large colonies at day 14 of culture. *Statistically significant (p <0.05). (D) Bright-field images and fluorescence micrographs of large colonies (containing more than 100 cells) transduced with indicated viruses at day 5 of culture. Dual immunostaining was performed to detect the expression of Alb (red) and CK7 (green) in clonal colonies. EGFP expression (upper panels) and nuclear DAPI staining (middle panels) are shown in the insets. Scale bar = 200 μm. (E) The percentages of Alb^{+}CK7^{-}, Alb^{-}CK7^{+}, Alb^{+}CK7^{+}, and Alb^{-}CK7^{-} cells in large colonies containing more than 100 cells were calculated at day 5 of culture. The average for 10 colonies is presented as the mean ± SD. *Statistically significant (p <0.05).

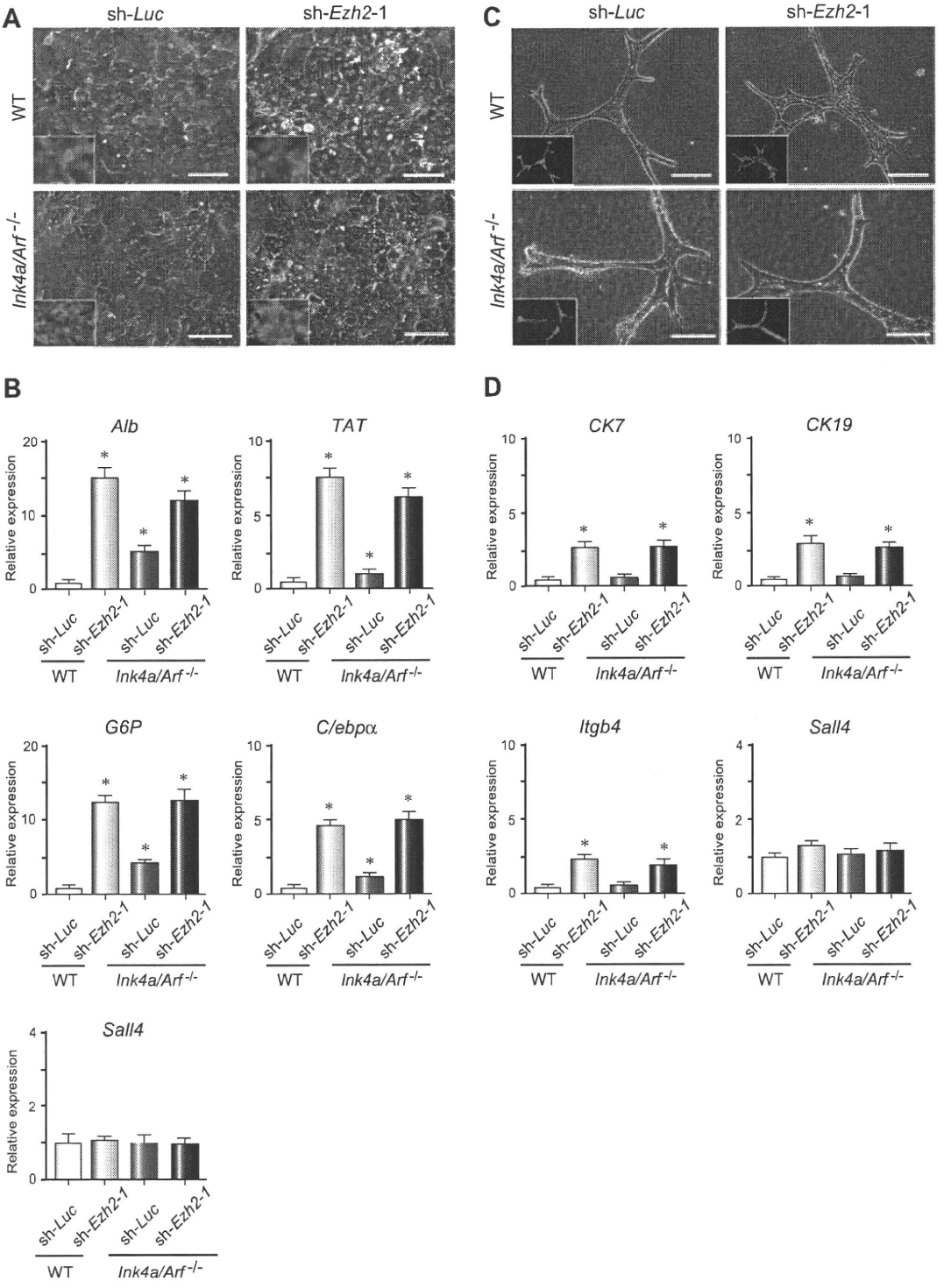

Fig. 6. Terminal differentiation of *Ezh2*-knockdown Dlk$^+$ cells towards hepatocytes and cholangiocytes. (A) To evaluate the terminal differentiation of wild-type or *Ink4a–Arf*$^{-/-}$Dlk$^+$ cells towards hepatocytes, *Ezh2*-knockdown Dlk$^+$ cells were placed on EHS gel in the presence of OSM. Bright-field images and fluorescence micrographs (inset panels) of cells in EHS gel at day 5 of culture are presented. Scale bar = 100 μm. (B) Real-time RT-PCR analyses of hepatocyte differentiation and maturation marker genes. *Statistically significant (p <0.05). (C) To evaluate the terminal differentiation of wild-type or *Ink4a–Arf*$^{-/-}$Dlk$^+$ cells towards cholangiocytes, *Ezh2*-knockdown Dlk$^+$ cells were subjected to collagen gel culture in the presence of TNF-α. Bright-field images and fluorescence micrographs (inset panels) of cells in collagen type I gel at day 5 of culture are presented. Scale bar = 100 μm. (D) Real-time RT-PCR analyses of cholangiocyte differentiation and maturation marker genes. *Statistically significant (p <0.05).

prevents the recruitment of liver-enriched transcription factors in hepatic stem/progenitor cells.

Although PcG proteins have been characterised as self-renewal factors of embryonic as well as somatic stem cells, Ezh2 has recently been implicated in the differentiation of neural stem cells and epidermal stem cells [12,13]. Our findings further support an essential role for PcG proteins in the precise regulation of stem cell differentiation. The composition of PcG complexes is highly dynamic and differs among different cell types and even at different gene loci. Given that the complexes exhibit differences in specificity for histone substrates, the target genes regulated by PcG proteins are quite diverse among different cell types [29]. Efforts to unravel the molecular machinery of PcG proteins, including Ezh2, would facilitate our overall understanding of the hepatic stem cell system and contribute to the establishment of liver regeneration therapy.

Conflicts of interest

The Authors who have taken part in this study declared that they do not have anything to disclose regarding funding or conflict of interest with respect to this manuscript.

Acknowledgements

The authors thank Dr. Kristian Helin for the anti-Ezh2 antibody, Dr. Hiroyuki Miyoshi for the CS-H1-shRNA-EF-1α-EGFP and CS-H1-shRNA-RfA-ERP vectors, Dr. Akihide Kamiya for technical assistance and Mieko Tanemura for laboratory assistance.

Financial support: This work was supported in part by grants for the Global COE program (Global Center for Education and Research in Immune System Regulation and Treatment) from the Ministry of Education, Culture, Sports, Science and Technology, Japan, and grants from the Core Research for Evolutional Science and Technology (CREST) of Japan Science and Technology Corporation (JST), the Takeda Science Foundation, and the Uehara Memorial Foundation.

Appendix A. Supplementary data

Supplementary data associated with this article can be found, in the online version, at doi:10.1016/j.jhep.2010.01.027.

References

[1] Fausto N. Liver regeneration and repair: hepatocytes, progenitor cells, and stem cells. Hepatology 2004;39:1477–1487.
[2] Tanimizu N, Nishikawa M, Saito H, Tsujimura T, Miyajima A. Isolation of hepatoblasts based on the expression of Dlk/Pref-1. J Cell Sci 2003;116:1775–1786.
[3] Tanimizu N, Hiroki S, Keith M, Miyajima A. Long-term culture of hepatic progenitors derived from mouse Dlk$^+$ hepatoblasts. J Cell Sci 2004;117:6425–6434.
[4] Pietersen AM, van Lohuizen M. Stem cell regulation by polycomb repressors: postponing commitment. Curr Opin Cell Biol 2008;20:201–207.
[5] Yonemitsu Y, Imazeki F, Chiba T, Fukai K, Nagai Y, Miyagi S, et al. Distinct expression of polycomb group proteins EZH2 and BMI1 in hepatocellular carcinoma. Hum Pathol 2009;40:1304–1311.
[6] Chiba T, Zheng YW, Kita K, Yokosuka O, Saisho H, Onodera M, et al. Enhanced self-renewal capability in hepatic stem/progenitor cells drives cancer initiation. Gastroenterology 2007;133:937–950.
[7] Kamiya A, Kinoshita T, Ito Y, Matsui T, Morikawa Y, Senba E, et al. Fetal liver development requires a paracrine, action of oncostatin M through the gp 130 signal transducer. EMBO J 1999;18:2127–2136.
[8] Nishikawa Y, Tokusashi Y, Kadohama T, Nishimori H, Ogawa K. Hepatocytic cells form bile duct-like structures within a three-dimensional collagen gel matrix. Exp Cell Res 1996;223:357–371.
[9] Negishi M, Saraya A, Miyagi S, Nagao K, Inagaki Y, Nishikawa M, et al. Bmi1 cooperates with Dnmt1-associated protein 1 in gene silencing. Biochem Biophys Res Commun 2007;353:992–998.
[10] Tzatsos A, Pfau R, Kampranis SC, Tsichlis PN. Ndy1/KDM2B immortalizes mouse embryonic fibroblasts by repressing the Ink4a/Arf locus. Proc Natl Acad Sci USA 2009;106:2641–2646.
[11] Oikawa T, Kamiya A, Kakinuma S, Zeniya M, Nishinakamura R, Tajiri H, et al. Sall4 regulates cell fate decision in fetal hepatic stem/progenitor cells. Gastroenterology 2009;136:1000–1011.
[12] Sher F, Roßler R, Brouwer N, Balasubramaniyan V, Boddeke E, Copray S. Differentiation of neural stem cells into oligodendrocytes: involvement of the polycomb group protein Ezh2. Stem Cells 2008;26:2875–2883.
[13] Ezhkova E, Pasolli HA, Parker JS, Stokes N, Su IH, Hannon G, et al. Ezh2 orchestrates gene expression for the stepwise differentiation of tissue-specific stem cells. Cell 2009;136:1122–1135.
[14] Oguro H, Iwama A, Morita Y, Kamijo T, van Lohuizen M, Nakauchi H. Differential impact of *Ink4a* and *Arf* on hematopoietic stem cells and their bone marrow microenvironment in *Bmi1*-deficient mice. J Exp Med 2006;203:2247–2253.
[15] Molofsky AV, He S, Bydon M, Morrison SJ, Pardal R. Bmi-1 promotes neural stem cell self-renewal and neural development but not mouse growth and survival by repressing the $p16^{Ink4a}$ and $p19^{Arf}$ senescence pathways. Genes Dev 2005;19:1432–1437.
[16] Bracken AP, Kleine-Kohlbrecher D, Dietrich N, Pasini D, Gargiulo G, Beekman C, et al. The Polycomb group proteins bind throughout the INK4A–ARF locus and are disassociated in senescent cells. Genes Dev 2007;21:525–530.
[17] Bernstein BE, Mikkelsen TS, Xie X, Kamal M, Huebert DJ, Cuff J, et al. A bivalent chromatin structure marks key developmental genes in embryonic stem cells. Cell 2006;125:315–326.
[18] Ku M, Koche RP, Rheinbay E, Mendenhall EM, Endoh M, Mikkelsen TS, et al. Genomewide analysis of PRC1 and PRC2 occupancy identifies two classes of bivalent domains. PLoS Genet 2008;4:e1000242.
[19] Pietersen AM, Horlings HM, Hauptmann M, Langerød A, Ajouaou A, Cornelissen-Steijger P, et al. EZH2 and BMI1 inversely correlate with prognosis and TP53 mutation in breast cancer. Breast Cancer Res 2008;10:R109.
[20] Chen H, Gu X, Su IH, Bottino R, Contreras JL, Tarakhovsky A, et al. Polycomb protein Ezh2 regulates pancreatic beta-cell Ink4a/Arf expression and regeneration in diabetes mellitus. Genes Dev 2009;23:975–985.
[21] Sasaki M, Yamaguchi J, Itatsu K, Ikeda H, Nakanuma Y. Over-expression of polycomb group protein EZH2 relates to decreased expression of p16 INK4a in cholangiocarcinogenesis in hepatolithiasis. J Pathol 2008;215: 175–183.
[22] Nagy P, Bisgaard HC, Thorgeirsson SS. Expression of hepatic transcription factors during liver development and oval cell differentiation. J Cell Biol 1994;126:223–233.
[23] Sund NJ, Ang SL, Sackett SD, Shen W, Daigle N, Magnuson MA, et al. Hepatocyte nuclear factor 3b (Foxa2) is dispensable for maintaining the differentiated state of the adult hepatocyte. Mol Cell Biol 2000;20: 5175–5183.
[24] Ishizaka S, Shiroi A, Kanda S, Yoshikawa M, Tsujinoue H, Kuriyama S, et al. Development of hepatocytes from ES cells after transfection with the HNF-3beta gene. FASEB J 2002;16:1444–1446.
[25] Ishii K, Yoshida Y, Akechi Y, Sakabe T, Nishio R, Ikeda R, et al. Hepatic differentiation of human bone marrow-derived mesenchymal stem cells by tetracycline-regulated hepatocyte nuclear factor 3beta. Hepatology 2008;48:597–606.
[26] Tan EH, Ma FJ, Gopinadhan S, Sakban RB, Wang ND. C/EBP alpha knock-in hepatocytes exhibit increased albumin secretion and urea production. Cell Tissue Res 2007;330:427–435.
[27] Zaret KS. Regulatory phases of early liver development: paradigms of organogenesis. Nat Rev Genet 2002;3:499–512.
[28] Boyer LA, Plath K, Zeitlinger J, Brambrink T, Medeiros LA, Lee TI, et al. Polycomb complexes repress developmental regulators in embryonic stem cells. Nature 2006;441:349–353.
[29] Kuzmichev A, Margueron R, Vaquero A, Preissner TS, Scher M, Kirmizis A, et al. Composition and histone substrates of polycomb repressive group complexes change during cellular differentiation. Proc Natl Acad Sci USA 2005;102:1859–1864.

Hepatology Research

Hepatology Research 2010; **40**: 415–423 doi: 10.1111/j.1872-034X.2010.00617.x

Original Article

Internal ribosomal entry-site activities of clinical isolate-derived hepatitis A virus and inhibitory effects of amantadine

Tatsuo Kanda, Fumio Imazeki, Shingo Nakamoto, Kohichiroh Okitsu, Keiichi Fujiwara and Osamu Yokosuka

Department of Medicine and Clinical Oncology, Graduate School of Medicine, Chiba University, Chiba, Japan

Aim: Little is known about specific naturally-occurring internal ribosomal entry site (IRES) activities of hepatitis A virus (HAV). We examined these activities using the bicistronic reporter assay and the effects of antiviral amantadine against their activities.

Methods: Six HAV IRES clones from three patients with fulminant hepatitis and three with self-limited acute hepatitis were obtained. The activities of their IRES were analyzed using bicistronic reporter assay in hepatocyte- and non-hepatocyte-derived cell lines, and the potential efficaciousness of the amantadine was examined.

Results: One clone from fulminant hepatitis had a deletion in domains III–IV of HAV IRES had higher IRES activities than HM175 in HLE and Huh-7 cells. In Huh-7 cells, amantadine is effective for inhibiting HAV IRES activities, and especially fulminant hepatitis-derived ones.

Conclusion: HAV IRES derived from clinical isolates have various activities. Bicistronic reporter assay using clinical isolates may be another useful tool for testing antiviral activities like those of amantadine and the new acridines and hydrazones recently reported.

Key words: amantadine, fulminant hepatitis, hepatitis A virus, hepatocyte, internal ribosomal entry site

INTRODUCTION

HEPATITIS A VIRUS (HAV) is a member of the genus *Hepatovirus* in the *Picornaviridae* family. HAV is a positive-sensed single-stranded RNA genome of approximately 7.5 kb in length. The genome codes a large open reading frame (ORF), which is flanked by 5′ non-translated region (5′NTR) and 3′NTR. The downstream part of 5′NTR represents the internal ribosomal entry site (IRES), which mediates cap-independent translation initiation.[1,2] HAV causes acute hepatitis and occasionally leads to severe fulminant hepatitis with fatal outcomes in unvaccinated individuals. Almost 3500 acute hepatitis cases were reported in 2006, representing an estimated 32 000 HAV cases annually in the USA.[3] HAV has dramatically affected rates of the disease in the USA. There continued to be missed opportunities for testing and/or vaccination, and so adherence to recommended HAV vaccination is still low.[4] This highlights the urgent need for a new therapeutic option other than vaccine.[5–10]

Picornavirus translation is initiated in a cap-independent fashion by a mechanism involving the binding of the 40S ribosomal subunit at a site located hundreds of bases downstream of the 5′ end of the RNA, which has been termed IRES. Although the details of translation initiation by internal entry are unknown, it likely involves the interaction of a set of *trans*-acting cellular translation initiation factors with the *cis*-acting IRES, resulting in the binding of the 40S ribosomal subunit to the RNA.[11] HAV IRES spans a region from nt. 161 to the first initiator, AUG, located at nt. 734, and encompasses most of 5′NTR of the viral mRNA.[12] In

Correspondence: Associate Professor Tatsuo Kanda, Department of Medicine and Clinical Oncology, Graduate School of Medicine, Chiba University, 1-8-1 Inohana, Chuo-ku, Chiba 260-8677, Japan. Email: kandat-cib@umin.ac.jp

This work was presented at the 13th International Symposium on Viral Hepatitis and Liver Disease, Washington DC, USA on 21 March 2009.

Received 11 May 2009; revision 14 September 2009; accepted 22 September 2009.

HAV genomes, the nucleotide sequence of 5'NTR is more conserved than those of other sites,[13,14] and 5'NTR is predicted to fold into a complex secondary/tertiary structure characterized by six major domains designated I–VI.[15] Domain VI contains the initiation codon. We previously showed that RNA interference targeting various domains of HAV IRES could suppress HAV translation and replication,[6] indicating that some HAV IRES domains might be used as a universal, effective target for specific inhibition of HAV infection.[6] HAV IRES could represent an appropriate target for antiviral drug development.

Amantadine is a tricyclic symmetric amine for use both as an antiviral and an anti-parkinsonian drug. Amantadine inhibits cell-culture-grown HAV IRES-mediated translation in human hepatoma cells,[7] supporting the observation that amantadine could suppress HAV replication in cell culture.[9,16–18] We do not know whether amantadine could suppress clinical isolates from hepatitis A patients.

Here, we examined the HAV IRES activities of clinical isolates from fulminant hepatitis and self-limited acute hepatitis patients in a number of cell lines and tested the effects of amantadine on their IRES-mediated translation by reporter assay. As translation of fulminant hepatitis-derived IRES varies, but it is still efficiently suppressed by amantadine, the approaches described here might open new strategies for useful therapeutic options in cases of fulminant hepatitis A.

METHODS

Cell lines and reagents

HUMAN HEPATOMA CELL lines Huh-7, HepG2 and HLE, the human cervical carcinoma cell line HeLa, and African green monkey kidney cell lines BSC-1 and CV-1 were purchased from Health Science Research Resources Bank (Japanese Collection of Research Bioresources, Osaka, Japan) and maintained in Dulbecco's minimum essential medium (Gibco BRL, Gaithersburg, MD, USA). Amantadine hydrochloride was purchased from Sigma-Aldrich (St Louis, MO, USA).

Bicistronic reporter plasmids

The simian virus (SV)40 promoter plasmid pSV40-HAV-HM175-IRES encodes in a bicistronic fashion the *Renilla reniformis* luciferase (Rluc), the HAV IRES derived from pHM175 (kindly provided by S. U. Emerson, National Institutes of Health, Bethesda, MD, USA),[19] followed by the firefly luciferase (Fluc). It was prepared by polymerase chain reaction (PCR)-based subcloning the IRES (nt. 139–854) of HAV strain HM175[19] and Rluc into pGL3-promoter Vector (Promega, Madison, WI, USA) (Fig. 1a, upper part). Plasmids pSV40-HAV-F1-IRES, pSV40-HAV-F2-IRES, pSV40-HAV-F3-IRES, pSV40-HAV-A1-IRES, pSV40-HAV-A2-IRES and pSV40-HAV-A3-IRES replaced HAV-F1-IRES, HAV-F2-IRES, HAV-F3-IRES, HAV-A1-IRES, HAV-A2-IRES and HAV-A3-IRES, respectively, into HAV-HM175 of the plasmid pSV40-HAV-HM175-IRES. F1–F3 and A1–A3 are derived from fulminant hepatitis and self-limited acute hepatitis, respectively.[20,21] The sequences of plasmids were confirmed by directly sequencing using ABI 377 (Applied Biosystems, Urayasu, Japan).

Transfection and *in vitro* reporter assays

Approximately 1.0×10^5 cells per well were placed in a six-well plate (Iwaki Glass, Tokyo, Japan) 24 h prior to transfection. Cells were transfected with 0.4 μg of pSV40-HAV-IRES using Effectene Transfection Reagent (QIAGEN, Hilden, Germany) following the manufacturer's protocol. Six hours after transfection, the cells were washed once with phosphate buffered saline (PBS), and culture media with or without drugs were added. Forty-eight hours after transfection, cells were harvested using reporter lysis buffer (Toyo Ink, Tokyo, Japan), and luciferase activity was determined by luminometer (AB-2200-R; ATTO, Tokyo, Japan).[7] To control for variations in transcription, IRES activity was assessed by measuring the ratio of *Renilla* and firefly luciferases. All samples were run in triplicate.

Data analysis

The sequences reported in this study have been deposited in GenBank under accession numbers AB513790 to AB513795 for F1 to A3. Sequence analyses were performed using GENETYX ver. 9 (GENETYX, Tokyo, Japan). Data were expressed as mean ± standard deviation. Statistical analysis was done using Student's *t*-test. $P < 0.05$ was considered significant.

RESULTS AND DISCUSSION

Naturally occurring HAV IRES

HEPATITIS A VIRUS strains associated with human disease show genetic divergence.[22,23] First, we cloned the sequences of HAV derived from clinical isolates and made each bicistronic vector. PCR products were derived from serum samples of patients with fulminant hepatitis, in whom prothrombin time had

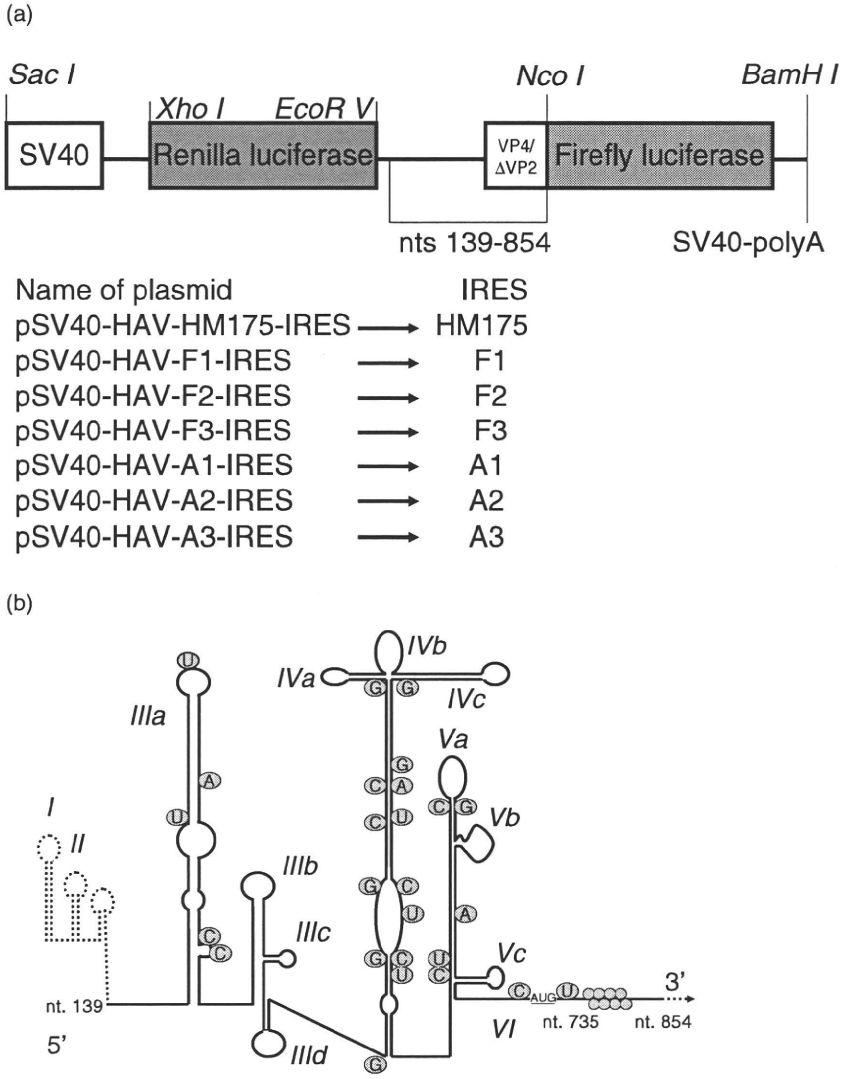

Figure 1 Bicistronic reporter constructs used in this study. (a) pSV40-HAV-HM175-IRES was described previously.[6,7] It encodes the *Renilla* luciferase genes, the internal ribosome entry site (IRES) of hepatitis A virus (HAV) HM175, and the firefly luciferase gene under the control of the simian virus 40 promoter (SV40). pSV40-HAV-F1-IRES, pSV40-HAV-F2-IRES, and pSV40-HAV-F3-IRES encode the IRES from fulminant hepatitis F1, F2, and F3, respectively, instead of the IRES of HM175. pSV40-HAV-A1-IRES, pSV40-HAV-A2-IRES and pSV40-HAV-A3-IRES encode the IRES from self-limited acute hepatitis A1, A2 and A3, respectively, instead of the IRES of HM175. (b–g) Secondary structure and mutations in the HAV IRES constructs used in this study.[6,7,11] Major structural domains are labeled I–VI; blue circles indicate mutations and red-dashed lines were deleted parts, compared with HM175 clone. HAV IRES constructs used in this study include the black line parts. F1 (b), F2 (c) and F3 (d) and A1 (e), A2 (f) and A3 (g) were derived from fulminant and acute self-limited hepatitis, respectively.

decreased to less than 40% with hepatic encephalopathy of grade II or more within 8 weeks after the onset of disease,[24] and with self-limited acute hepatitis in whom prothrombin time had not decreased below 40%. We sequenced these isolates, showing the differences of these sequences in Figure 1(b–g). Of note, one was derived from fulminant hepatitis F3 with a sequence deletion from nt. 233–380 in the HAV IRES region (Fig. 1d) corresponding to a portion of domain III to a part of domain IV. This F3 nucleotide sequence matched 75.60–77.93% of those of cell culture-derived clone HM175 or other clinical isolates in this study. The

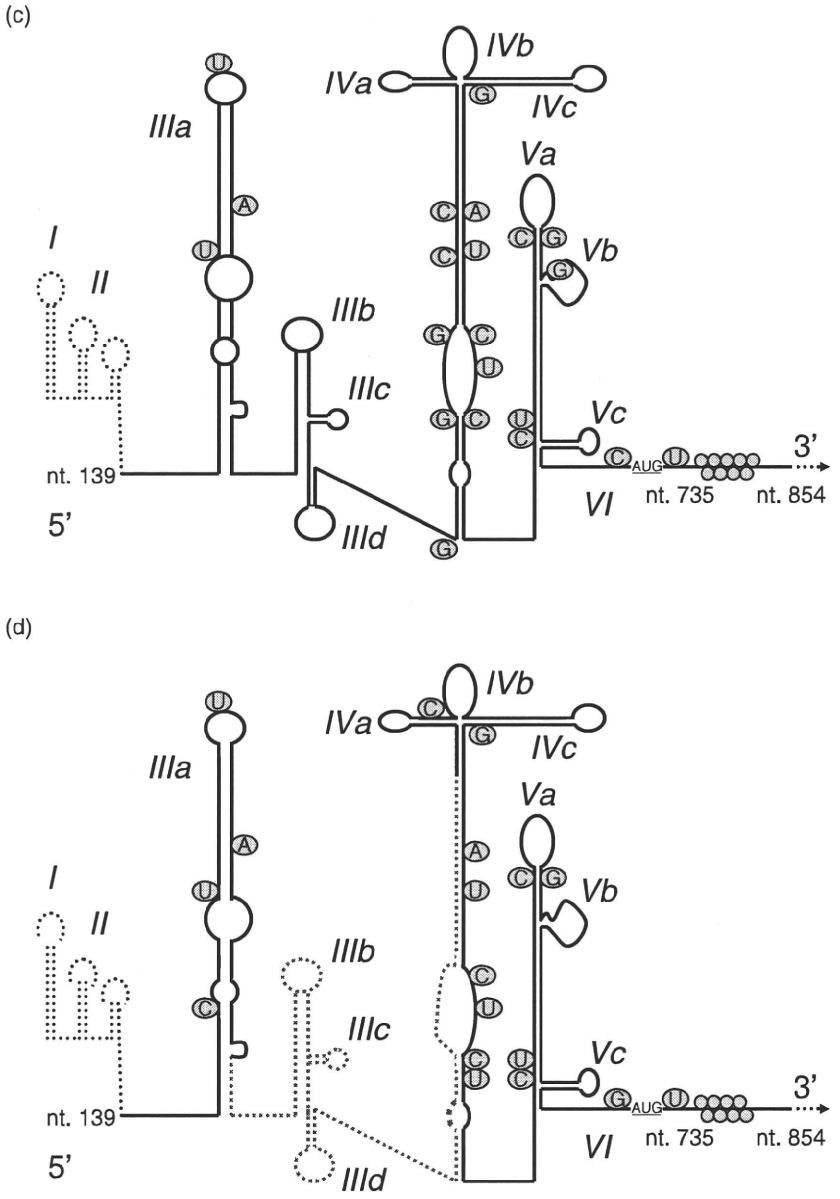

Figure 1 *Continued.*

nucleotide sequences of other clinical isolates matched 95.25–95.81% of that of HM175. The ones other than F3 matched 98.18–99.30% with each other (data not shown).

HAV IRES activities from clinical isolates vary in human hepatocytes

Several mutational studies of HAV IRES were previously reported.[25,26] Our major concern before starting this study was whether HAV IRES activities were correlated to the severities of the clinical manifestations of hepatitis A, as HAV genome replication is directly dependent on IRES-mediated translation. Then, we examined how these IRES activities behaved in hepatocytes and non-hepatocytes. It is thought that HAV mainly replicates in the liver where it induces inflammation,[1,2] so we initially examined translation efficiencies of HAV IRES in the following human hepatoma cells: Huh-7, HepG2 and HLE cells (Fig. 2a–c). The IRES activities (firefly luciferase/*Renilla* luciferase: cap-independent/cap-